Cyclotrons

R. Baartman, T. Planche

November 19, 2020

Contents

Chapter 1

Why Cyclotrons?

A particle accelerator is a device that uses electromagnetic fields to bring particles to high energies while keeping them organized. The magnetic fields are the most efficient way to control particle bunches and keep them focused, but the Lorentz force law shows that actual acceleration that increases the particles' energy requires time-varying electric fields. In some accelerators, the magnetic field is increased to keep the particles' trajectories unchanged as they accelerate, but in others, the magnetic field is fixed and the orbit allowed to change. Cyclotrons are of the latter type. We will not review all the types, but the summary is in the table. (Show fixed/varying field, fixed/varying frequency, multipass/singlepass, maybe one of Werner Joho's.) Because of this feature, cyclotrons do not have an easy description for the particle optics properties. Let us look at this in more detail.

In a synchrotron, there is one fixed closed orbit and the particles' motion can be described with reference to that orbit. Therefore, the difference between an arbitrary particle's coordinates and the reference trajectory transverse coordinates is small, and in a properly designed machine, it remains small. The energy difference between typical particles on that orbit is small, typically a percent or less. This allows a tremendous simplification because all the optics can be understood on the basis of a Taylor expansion. The lowest order effects are linear and the accelerator is designed in such a way that they dominate. When they do, all the optics is linear and can be described by matrices. The beam accelerates but, because the orbits are fixed, the transverse dynamics are also fixed; in particular, the "tunes" are fixed.

Conversely, in a cyclotron, in general, the orbits are not closed in space. The trajectory is a continuous spiral, so there can be particles simultaneously in the tank that have momentum differing by one or two orders of magnitude. There is no hope of a useful Taylor expansion in that case. Nevertheless, it is still possible to design transverse motion that is linear. The

technique is to find a closed orbit at any energy and expand transverse coordinates about it. The character of this closed orbit changes as a function of energy, so the "tune" is not fixed.

It is possible to design a cyclotron with exactly the same closed orbits through all of the up to 2 orders of magnitude momentum change, by scaling the orbit shape. But then its isochronism is lost and the chief advantage is also lost. It is still a "fixed field accelerator" (FFA), but because of the non-isochronous character, the frequency of the acceleration cavities must change to follow the revolution frequency of the particles as they accelerate. And thus the machine is pulsed, losing its continuous (linac-like) character. Pulsed, there is a loss of a factor of 100 to 1000 in intensity because the machine can tolerate only one turn at a time.

It is the chief advantage of cyclotrons over other accelerators that the particles use the same rf electric field turn after turn and yet they do not require pulsing and the inherent orders of magnitude loss in time averaged intensity. The linac is a counter example: each particle sees each acceleration gap only once. Although capable in principle of operating cw, linacs, even superconducting ones are pulsed to minimize power consumption. Typically a room temperature linac needs orders of magnitude more "wall plug power" than the beam power that is output. Not so with cyclotrons; there are cases where the wall plug power is only factor of 2 or 3 more than the output beam power. See Humbel et al.[1]; the final sentence states: *"The upgraded PSI Ringcyclotron will convert 60% of wall plugged power consumption into net beam power"*. This is because in a typical cyclotron, there are a few hundred to a few thousand turns. An individual cyclotron accelerating cavity will see a beam current of the output current ($\sim 1\,\mathrm{mA}$ is currently state of the art) multiplied by this number of turns, thus on order of 1 Ampere. This is comparable to the generator current used to drive the cavity and results in high efficiency but also large beam loading effects.

Chapter 2

How Cyclotrons?

2.1 Isochronous orbits

As the particles in a cyclotron speed up, they also are forced to take longer orbits. The magic of the cyclotron is that it is tuned to exactly cancel the two effects, and therefore the orbit period remains constant and the beam can be accelerated continuously without pulsing. Historically, this was first capiltalized upon by Ernest Lawrence[2]. At low energy, where particles have little kinetic energy, this is the simplest to understand. As the transverse force exerted by the vertical magnetic field is qvB, continuously at right angles to the particle's speed v, the particles travel in circles of radius $\mathcal{R}$ given by

$$\frac{mv^2}{\mathcal{R}} = qvB, \text{ or, } m\omega = qB \tag{2.1}$$

the frequency of revolution is fixed, independent of energy, if magnetic field is fixed and uniform.

2.2 But ... focusing

The fixed frequency means that we can accelerate by providing an electric field with for example a high Q cavity, allowing to reach high energy using relatively low voltage and low power, and no pulsing. For example and typically, 100's of MeV is achieved using voltages of only 10's of kV. The total path length of particles through a cyclotron can be 10's of km! Clearly, the particles must stay transversely controlled over such long distance. In other words, besides guiding the particles in circles (spirals to be precise), we also need to focus them toward the desired orbits. In the horizontal direction, this

is not an issue as the fact of circular orbits automatically implies containment in that direction. But the concern is vertical motion. The simplest way to achieve forces toward the median plane of the magnet is to have the magnetic field lines bulging as seen in the figure. Particles receding need to be forced to the right in the figure, and approaching particles to the left. Bulging lines will mean there is also a slight force toward the median plane. Let us use Maxwell equation to determine what this means.

The "bulging" means there is a radial component $B_{\mathcal{R}}$, and the vertical resulting force is $F_z = qvB_{\mathcal{R}}$. This needs to be linear, with zero force on the mid-plane ($z = 0$), so in the Taylor-expansion $F_z = qv\frac{\partial B_{\mathcal{R}}}{\partial z}z$. But knowing that $\nabla \times B = 0$, we also have $\frac{\partial B_{\mathcal{R}}}{\partial z} = \frac{\partial B_z}{\partial \mathcal{R}}$, so finally

$$F_z = qv\frac{\partial B_z}{\partial \mathcal{R}}z. \tag{2.2}$$

There is only a force toward the plane, and simple harmonic motion about it, if $\frac{\partial B_z}{\partial \mathcal{R}} < 0$; the field must be **falling** with radius and thus cannot be entirely isochronous.

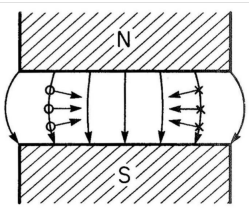

Figure 2.1: Azimuthally uniform field arrangement to provide vertical focusing.

2.2.1 Tunes

Traditionally, dipoles were characterized by a field index κ defined by $\kappa = \frac{\mathcal{R}}{B}\frac{dB}{d\mathcal{R}}$. If κ is constant, we have $B \propto \mathcal{R}^\kappa$: the orbits at different momenta are scaled versions of each other. We can rederive the focal properties from the well-known transfer matrix of a dipole.[3] For both radial and vertical motion, the transfer matrix can be written as

$$\begin{pmatrix} \cos kL & \frac{\sin kL}{k} \\ -k\sin kL & \cos kL \end{pmatrix}, \tag{2.3}$$

where L is the length of the arc in the dipole, and $k^2 = k_x^2 := (1+\kappa)/\mathcal{R}^2$ for radial motion, and $k^2 = k_z^2 := -\kappa/\mathcal{R}^2$ for vertical. Again, if κ is negative, the particles are vertically focused; if positive, k_z is imaginary and the matrix becomes, with now $k^2 = -k_z^2 = \kappa/\mathcal{R}^2$,

$$\begin{pmatrix} \cosh kL & \frac{\sinh kL}{k} \\ k\sinh kL & \cosh kL \end{pmatrix}. \tag{2.4}$$

We can derive tunes now. The *tune* is the number of oscillations per turn; this is reflected in the argument of the cosine, kL. One turn means $L = 2\pi\mathcal{R}$, so the number of oscillations per turn is $\nu = kL/(2\pi) = k$. So we can read off the tune:

$$\nu_x = \sqrt{1+\kappa},\ \nu_z = \sqrt{-\kappa}. \tag{2.5}$$

Notice that $\nu_x^2 + \nu_z^2 = 1$: plotted on a tune diagram, the tunes are confined to the unit circle.

2.2.2 Isochronism and Relativity Incompatible?

But that was for non-relativistic motion; for relativistic, the situation is worse; relativity requires the field to be **rising** with radius. This can be seen simply knowing only that rigidity, $B\mathcal{R} = p/q$ where p is the relativistically-correct definition of momentum: γmv. So now we have

$$\gamma m\omega = qB, \tag{2.6}$$

and this is only satisfied for fixed ω if $B \propto \gamma$. Since $\omega = v/\mathcal{R}$, we must have $\mathcal{R} \propto \beta$. Thus B is a function of $\mathcal{R}$ the same way that γ is a function of β. Let's be explicit:

$$B(\mathcal{R}) = \frac{B_{\rm c}}{\sqrt{1-\beta^2}} = \frac{B_c}{\sqrt{1-(\mathcal{R}/\mathcal{R}_\infty)^2}}, \tag{2.7}$$

where $B_c := \frac{m\omega}{q}$ and $\mathcal{R}_\infty := c/\omega$. These constants are fundamental to cyclotron design, as will be seen.

But the field index for isochronism is $\kappa = \frac{\mathcal{R}}{B}\frac{dB}{d\mathcal{R}} = \frac{\beta}{\gamma}\frac{d\gamma}{d\beta} = \beta^2\gamma^2 \neq$ constant. So isochronism requires the field to be non-scaling with radius. The tunes (2.5) in an isochronous machine would be:

$$\nu_x = \sqrt{1+\kappa} = \gamma,\ \nu_z = \sqrt{-\kappa} = \beta\gamma i, \tag{2.8}$$

so there is no vertical stability.

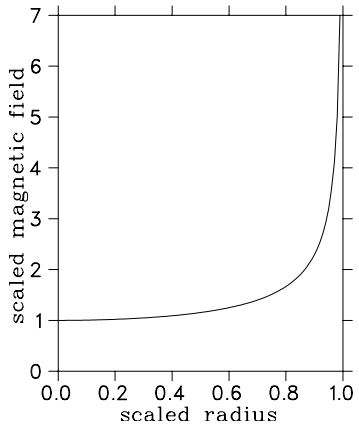

Figure 2.2: Average magnetic field versus orbit length /2π.

Now, since the early 50s, we know the trick of strong focusing and therefore it seems obvious that we can add and take away focusing by splitting the magnet into sectors and using the edges of the sectors for focusing.

But first: How does the isochronism condition change if B is not uniform? Let us define θ to be the angle of the reference particle momentum with respect to the lab frame. Orbit length L is given by speed and orbit period T:

$$L = \oint ds = \oint \mathcal{R}d\theta = \beta cT. \tag{2.9}$$

The local curvature $\mathcal{R} = \mathcal{R}(s)$ can vary and for reversed-field bends even changes sign. (Along an orbit, $ds = \mathcal{R}d\theta > 0$ so $d\theta$ is also negative in reversed-field bends.) Of course on one orbit, we always have

$$\oint d\theta = 2\pi. \tag{2.10}$$

What is the magnetic field averaged over the orbit?

$$\overline{B} = \frac{\oint B ds}{\oint ds} = \frac{\oint B\mathcal{R}\, d\theta}{\beta c T}. \tag{2.11}$$

But $B\mathcal{R}$ is constant on a closed orbit and in fact is $\beta\gamma mc/q$. Therefore we see that the original equation (2.7) is maintained with B replaced by its average, and $\mathcal{R}$ redefined as orbit length divided by 2π.

$$\overline{B} = \frac{2\pi}{T}\frac{m}{q}\gamma \quad \equiv B_{\rm c}\,\gamma = \frac{B_{\rm c}}{\sqrt{1-(\mathcal{R}/\mathcal{R}_\infty)^2}}. \tag{2.12}$$

This shows that isochronism does not require the field to be uniform on an orbit; it can vary by any amount provided the average is correct. What's also not obvious is that this can benefit vertical stability without significantly changing horizontal.

2.3 Edge Focusing

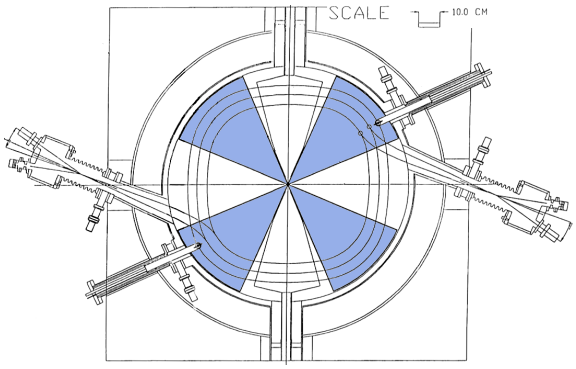

Figure 2.3: TR13 cyclotron showing "Thomas focusing" resulting from orbits crossing sector edges at non-normal angles. Sectors are indicated in blue. The three orbits shown are 11, 14, and 17 MeV.

Look at Fig. 2.3. Here, as example, the magnetic field has been split into four sectors. Let the angular width of a sector be θ, and let there be in general N sectors. Then each sector must bend the orbit by $\phi := 2\pi/N$, so the orbit enters and exits each sector at an "edge" angle of

$$\alpha = \frac{1}{2}(\phi - \theta). \tag{2.13}$$

(This is most easily seen by following the orbit from midpoint of sector to the edge: orbit angle changes by π/N, the radial vector changes angle by $\theta/2$.) To find the optics, we just multiply the known transfer matrices together under the simplifying assumption that the field between sectors is zero, and that the magnet gap is small compared with the bend radius. From the start of a sector, we have: Edge, Sector, Edge, Drift so the matrices (reading as they do right to left) for respectively horizontal motion and vertical motion, M_x, M_z, are as follows:

$$M_x := \begin{pmatrix} 1 & d \\ 0 & 1 \end{pmatrix} \begin{pmatrix} 1 & 0 \\ \frac{1}{f} & 1 \end{pmatrix} \begin{pmatrix} \cos[k_x s] & \sin[k_x s]/k_x \\ -k_x \sin[k_x s] & \cos[k_x s] \end{pmatrix} \begin{pmatrix} 1 & 0 \\ \frac{1}{f} & 1 \end{pmatrix} \tag{2.14}$$

$$M_z := \begin{pmatrix} 1 & d \\ 0 & 1 \end{pmatrix} \begin{pmatrix} 1 & 0 \\ -\frac{1}{f} & 1 \end{pmatrix} \begin{pmatrix} \cosh[k_z s] & \sinh[k_z s]/k_z \\ k_z \sinh[k_z s] & \cosh[k_z s] \end{pmatrix} \begin{pmatrix} 1 & 0 \\ -\frac{1}{f} & 1 \end{pmatrix} \tag{2.15}$$

The signs are such that the sectors focus radially because of a field index needed for isochronism, and the edges defocus radially, while the sectors defocus vertically and the edges focus.

The focal length f of the magnet edges can be read from Brown[3] as:

$$\frac{1}{f} = \frac{\tan\alpha}{\rho}. \tag{2.16}$$

The orbit length in the dipole is $s = \rho\phi$. Let us define the "average radius" R of the orbit by the total length of the orbit in the sector period $d + s$:

$$\frac{2\pi R}{N} = d + s, \text{ or, } \phi = \frac{d+s}{R}. \tag{2.17}$$

For synchrotrons, $\frac{s}{d+s} = \frac{\rho}{R}$ is often called the "packing factor" as it is the fraction of the orbit occupied by dipoles. But here we use a different notation in line with historic development of cyclotrons. We define a parameter $F^2 = \frac{R}{\rho} - 1 = \frac{B}{\overline{B}} - 1$. In the general case, where dipoles do not have hard edges and the valleys do not have zero field but the field varies smoothly over an orbit, F is the fractional root mean-squared variation of the magnetic field:

$$F^2 = \frac{\overline{(B - \overline{B})^2}}{\overline{B}^2}. \tag{2.18}$$

The parameter F is known as the "flutter".

Lastly, the field index needed in the sector dipoles is found from the isochronism condition given above. Near the orbit the average field must vary with radial displacement x as $\overline{B}(x) = \overline{B}_0\left(1 + \frac{\kappa}{R}x\right)$ where $\kappa = \beta^2\gamma^2$. So inside the dipole, the local field index is

$$k = \frac{\rho}{R}\kappa. \tag{2.19}$$

Referring again to Brown[3], we have:

$$k_x = \frac{\sqrt{1+k}}{\rho} \text{ and } k_z = \frac{\sqrt{k}}{\rho}. \tag{2.20}$$

We put these together and extract the phase advance per cell as the arcosine of the half-trace. Expressed as a power series in ϕ, we then divide by ϕ to get the tune. The results are

$$\nu_x^2 = 1 + \kappa \quad \text{(which for isochronous)} \quad = \gamma^2, \tag{2.21}$$

$$\nu_z^2 = -\kappa + F^2 \quad \text{(which for isochronous)} \quad = F^2 - \beta^2\gamma^2. \tag{2.22}$$

There are two interesting results for isochronous machines: $\kappa = \beta^2\gamma^2$, $\nu_x = \gamma$, and the cyclotron will not work unless $F > \beta\gamma$. The former effect, that the horizontal tune is γ, means that high energy cyclotrons cannot avoid betatron resonances.

The latter result means for the example of the cyclotron pictured above, where $F \approx 1/2$, $E < 111\,\mathrm{MeV}$ for protons. Considering that cyclotrons had been topping out at about 12 MeV (see Bethe[4]), this was encouraging. This is known as "Thomas focusing" after LH Thomas as he was first to propose what is generally called "azimuthally-varying field" (AVF) cyclotrons[5].

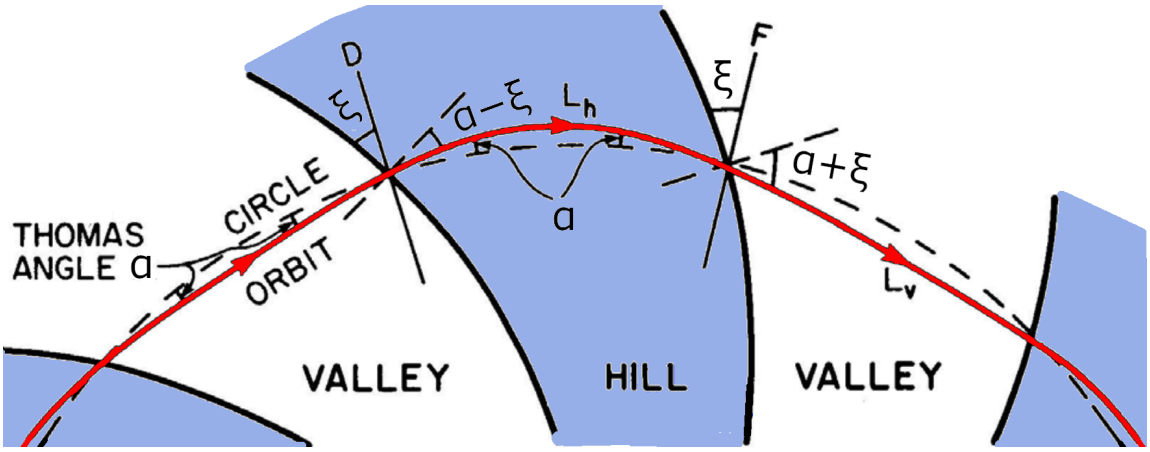

Figure 2.4: Spiralled sectors, defining spiral angle ξ, and Thomas angle α.

2.3.1 Strong Focusing

Of course, F can be made far larger by alternating the field gradient (or field index) sector to sector; isochronism constrains only the average gradient. Clearly, though, one needs more normal-index than reverse-index and this will make the cyclotron much larger than otherwise to achieve the required average field in spite of having reverse fields. But Donald Kerst[8, 9], realized that reversed fields are not at all needed to achieve strong focusing: one simply spirals the magnet sectors, see Fig. 2.4 thus adding thin lenses at the dipole edges that alternate in sign. To include this effect is straightforward: we simply replace the edge matrices' f with two different values, f_- for dipole entry, and f_+ for exit:

$$\frac{1}{f_\pm} = \frac{\tan(\alpha \pm \xi)}{\rho}, \tag{2.23}$$

where ξ is the spiral angle. The new tunes to lowest order in ϕ are:

$$\nu_x^2 = 1 + \kappa \quad \text{and} \quad \nu_z^2 = -\kappa + F^2(1 + 2\tan^2\xi). \tag{2.24}$$

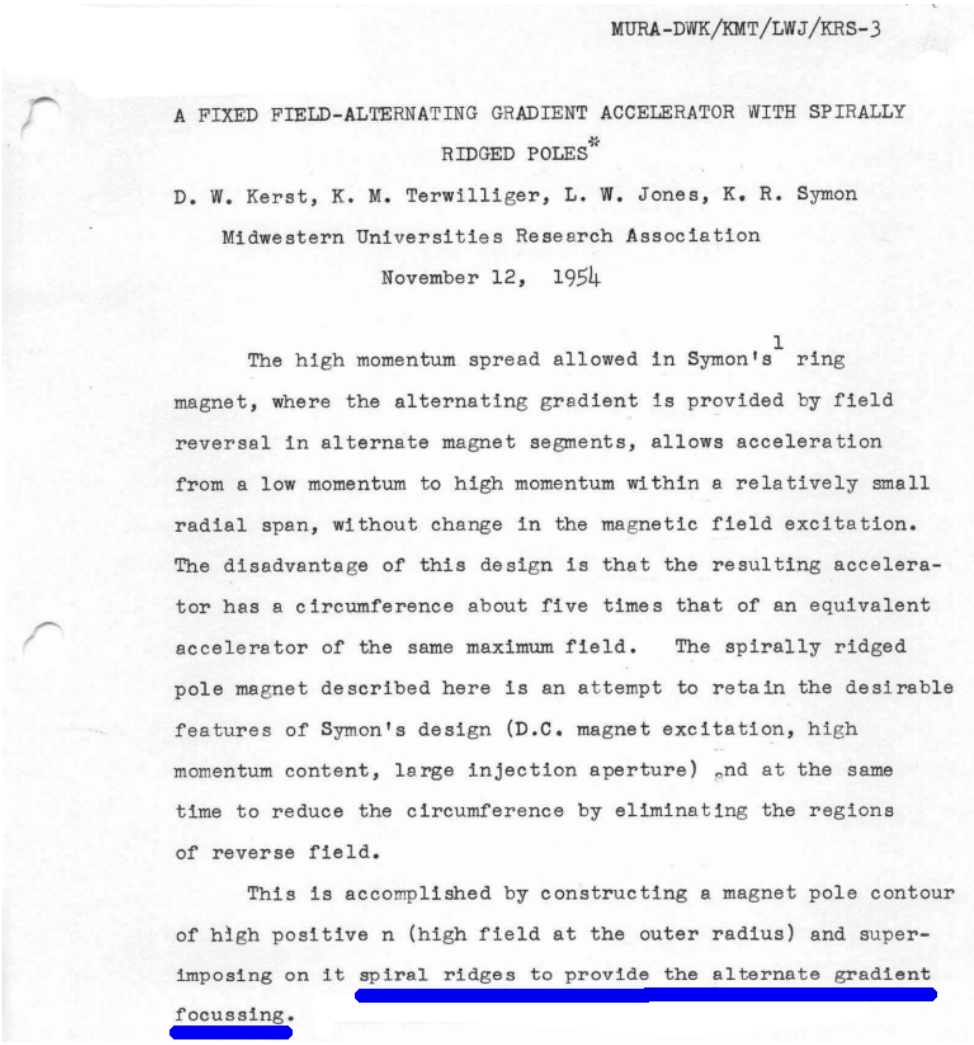

MURA-DWK/KMT/LWJ/KRS-3

A FIXED FIELD-ALTERNATING GRADIENT ACCELERATOR WITH SPIRALLY RIDGED POLES*

D. W. Kerst, K. M. Terwilliger, L. W. Jones, K. R. Symon
Midwestern Universities Research Association

November 12, 1954

The high momentum spread allowed in Symon's[1] ring magnet, where the alternating gradient is provided by field reversal in alternate magnet segments, allows acceleration from a low momentum to high momentum within a relatively small radial span, without change in the magnetic field excitation. The disadvantage of this design is that the resulting accelerator has a circumference about five times that of an equivalent accelerator of the same maximum field. The spirally ridged pole magnet described here is an attempt to retain the desirable features of Symon's design (D.C. magnet excitation, high momentum content, large injection aperture) and at the same time to reduce the circumference by eliminating the regions of reverse field.

This is accomplished by constructing a magnet pole contour of high positive n (high field at the outer radius) and superimposing on it spiral ridges to provide the alternate gradient focussing.

Figure 2.5: Kerst and other MURA authors presenting Kerst's invention of spiralled sector to incorporate strong focussing in an efficient manner. As a historical note, it is worth pointing out that "alternating gradient" focussing and "strong focussing" are now used interchangably and the invention is usually attributed to Ernest Courant[6]. The older "alternating gradient" appellation is explained by the fact that all accelerators up to and including the CERN PS and Brookhaven AGS used only dipoles with field indexes. Quadrupoles were invented by Toshio Kitagaki in 1952[7] and did not "catch on" immediately. But the older name still applies: whether the focussing comes from dipoles with alternating field indexes, spiralled dipole edges, or quadrupoles of alternating polarity, in all three cases, there is a transverse gradient that alternates in sign.

This illustrates dramatically the "strength" of strong focusing. At a spiral angle of 66°, it is 10 times stronger than the 'Thomas' focusing. The TRIUMF cyclotron has been running > 40 years with a spiral angle $\xi = 70°$. Using this along with $F \sim 1$ as in the above radial sectored TR13 cyclotron, we see that the second term in equation 2.24 is 16. This would allow a proton machine to reach 3 GeV.

In fact there are designs to 15 GeV that use reverse-field "gulleys"[10], but nothing higher than 590 MeV has been built. By carefully balancing flutter and spiral angle, it's possible to maintain the vertical tune between integers. But the horizontal tune is still γ in this simple analysis, so it is difficult to avoid radial integer resonances when exceeding ~ 1 GeV for protons.

An example of a 2 GeV, 4 MW proton cyclotron[11] is shown schematically in Fig. 2.6. A more recent design (2016)[12] for 2 GeV, 3 mA or 6 MW power, uses reverse bends instead of relying solely on flutter and spiral angle. This results in a ring twice larger in diameter.

2.4 Longitudinal motion

The accelerating field need not be at the circulating frequency, but can be any integer multiple. For example the TRIUMF cyclotron operates at 5 times the revolution frequency: 23 MHz, where the revolution is 4.6 MHz. This "harmonic number" (h) is determined in a way unrelated to the requirements for beam focussing. (More on this later.) $h = 4$ is typical. So there may be up to order of 10^3 to 10^4 rf periods in the history of one particle from injection to extraction. A net phase slip of 90° would cause the particle to stall, and anything larger would cause it to begin to decelerate. To take maximal advantage of this increase in efficiency, the cyclotrons that are designed to use stripping for extraction can have phase acceptances that are very large; up to 60°. So clearly it would be necessary to limit the phase slip to less than 60°, and in must cases for reasons of stability, it is desirable to limit the slip to less than a tenth of this level. The tolerance in both frequency and magnetic field variation is thus in the range of one part in 10^5.

Cyclotrons that do not use stripping or other non-Liouvillean technique to extract require that the turns be separated or separable at the extraction energy. This puts a lower bound on the energy gain per turn and thus the rf cavity voltage. Further, it puts a severe restriction on the phase acceptance or the phase width of the particle bunches. As the particles are "frozen", fixed in place with respect to each other, the extreme phase particle of phase $\hat{\phi}$, receiving a factor $\cos\hat{\phi}$ with respect to the maximum energy gain, must satisfy $1 - \cos\hat{\phi} < 1/N_t$, where N_t is the number of turns. For example, this would be $\pm 3.6°$ for 500 turns: an order of magnitude down from H^- cyclotrons. Space charge forces modify

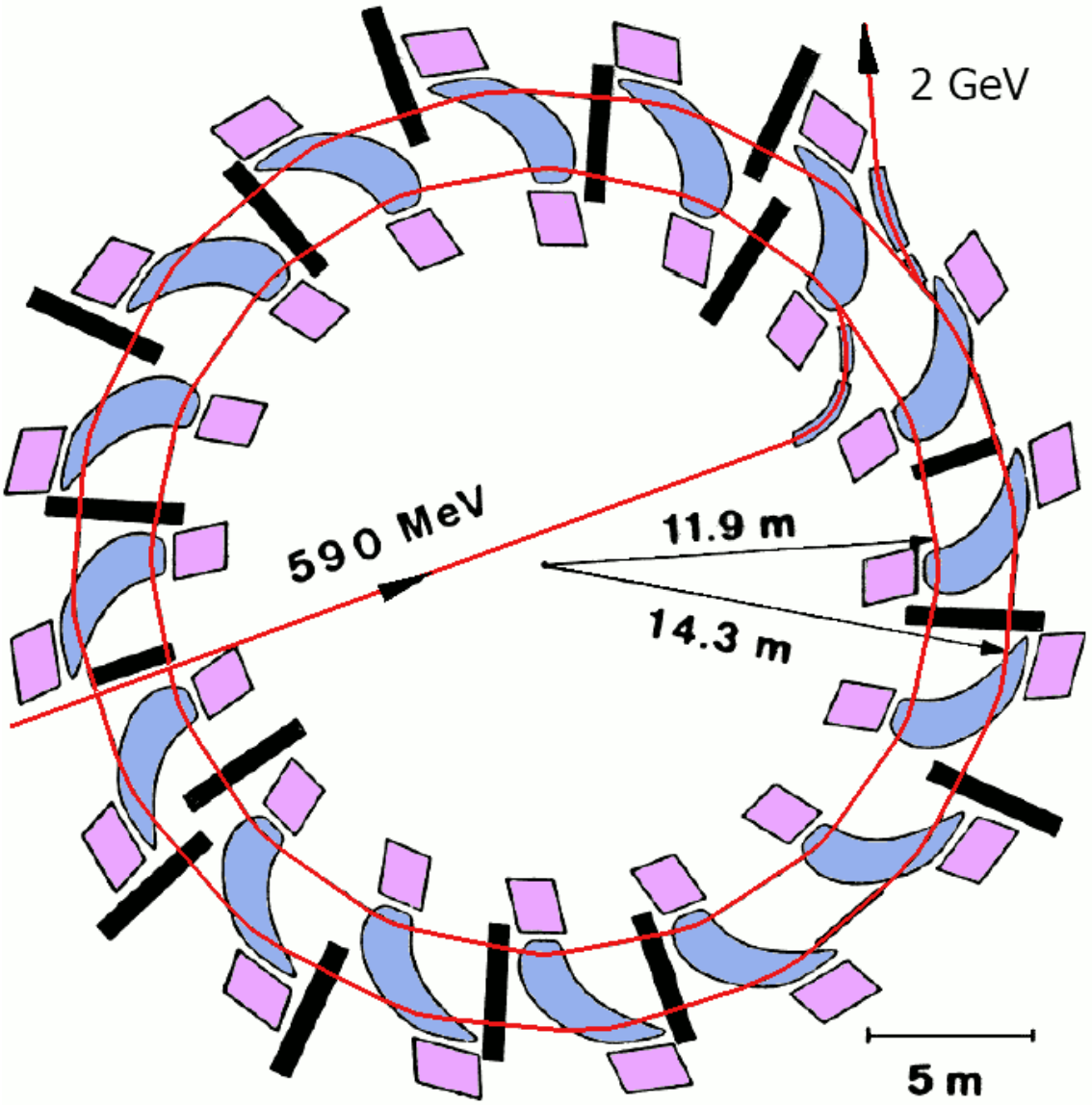

Figure 2.6: Proton cyclotron for 2 GeV, injecting at 590 MeV, devised by Werner Joho[11]. Injection and extraction orbits are indicated (red). The components are dipoles in light blue and their yokes in pink, and rf cavities in black. These components are similar to those that exist for the PSI 590 MeV cyclotron, which currently produces 2.4 mA protons.

this picture, and surprisingly relax the requirement; this will be dealt with in a later chapter.

2.4.1 Separated orbits?

Though cyclotrons operate on the basis of global isochronism (2.12), it does not actually follow that local isochronism is also required. In a manner analogous to a Fresnel lens, the local field derivative can be detached from the global average requirement. This requires that the orbits be individually confined, but on the other hand, local non-isochronicity allows longitudinal focusing. Just as in a synchrotron, if we are free to choose local gradients, we can set them to give not only the desired transverse tunes, fixed versus energy, but also the longitudinal tune. Such a machine is referred to as a Separated Orbit Cyclotron (SOC). It has been proposed a few times in the past[13, 14, 15], but none came to full fruition. The difficulty is that the individual orbits must be as stable as in a separated turn cyclotron and also of quality sufficient to maintain the emittance, and this requires highly accurate fields over a width that is large compared with the magnet gap, and this in turn means that the turn separation be large compared with the magnet gap. In effect, an SOC is much like a kilometres-long linac wound into a spiral, with optics that are in the less than 1 cm range, but without direct access to the orbits themselves for insertion of diagnostics and other tuning aids. It still has the advantage of particles re-using the acceleration field turn after turn, but the robustness and tuning simplicity of the simple cyclotron are lost.

Exercise: We have ignored dispersion in the transfer matrix. Find the average dispersion, knowing how energy increases with radius, and find the periodic dispersion for the case with dipoles and drifts.

Exercise: Read [16]. Find the increment in x and p_x at a cavity gap in an isochronous cyclotron. Remember, cyclotrons have $D/\rho = 1/\gamma^2$. Does this agree with calculation based upon radius gain per turn?

2.5 So what makes cyclotrons so different?

Modern synchrotrons' optics consist mainly of dipoles and quadrupoles. Why are cyclotrons so different? In particular, why not use quadrupoles in cyclotrons? The reason is that the transverse range needed to accommodate the accelerating particles in the fixed field is large, far larger than in synchrotrons, and in particular is generally very large compared with the magnet gap. Example: the TRIUMF cyclotron injects at 300 keV ($\beta\gamma = 0.025$), and extracts at 500 MeV ($\beta\gamma = 1.16$), a factor in momentum of 46! The TR30 cyclotron injects

at 25 keV and extracts at 30 MeV, a range of a factor 35. This is an essential difference from synchrotrons, which need accommodate a momentum range of only a few percent.

As well, for a cyclotron to accelerate up to desired energy, it will require that the isochronism condition (2.12) be met to an accuracy of one part in 10^4 to 10^5 over its complete momentum range of a factor 30 or more. This is far more stringent than the tolerance on synchrotron magnets. As a result, cyclotrons cannot be designed except at the very initial conceptual stage using "standard" optics codes and matrix multiplication.

In a cyclotron there is no fixed reference orbit. The particles spiral outward as they are accelerated in the fixed magnetic field. There is a fixed closed orbit for any energy, but the energy is increasing continuously. In synchrotrons also, there is a momentum acceptance range, but it is only of order a few percent. Within this range, one can find a closed orbit for any momentum; they scale according to a parameter called the periodic dispersion. In the synchrotron case all particles circulating are referenced to the closed reference trajectory, and their deviations of all six phase space coordinates from the reference particle are sufficiently small that all optics can be derived from a low order Taylor expansion. In cyclotrons, there is no hope for this kind of approach. Circulating particles cannot be thought of as being in orbits that are scalable or otherwise derivable from each other. The closed orbits' shapes depend on energy; tunes change by as much as a factor of 2; Twiss (Courant-Snyder[17]) β-functions change by a factor as large as 40 if starting from non-relativistic energy, since $\beta_{x,z} \propto R \propto v/c$. But in a synchrotron, they remain constant as the particles accelerate.

However, taking one energy at a time and its closed orbit, can we not continue to analyze the motion as in the example cyclotron in Fig. 2.5 above? No; those dipoles are highly idealized, with constant fields along the closed orbit and hard edged dipoles and zero field between dipoles, and only in this case do we know the reference orbit *a priori*: one can determine it with a ruler and compass and some trigonometry. In general, though, none of these characteristics are realistic even as approximations.

The closed orbit is not known. Consider that inside synchrotron magnets, even if combined function, the reference trajectory is known, closed, and the magnetic field along this trajectory is constant.[1] But even if a cyclotron consists of simple pie-sector-shaped dipoles, with field index $B(R) = B_0 R^k$, the closed orbits do not follow a constant R in the dipoles (see Fig. 2.3). Over the orbits, B and k are both varying and so the `TRANSPORT` standard dipole transfer matrices would be only approximately applicable.

A technique developed in the 50s and still in use today is to find the constant energy closed orbits for any given energy or momentum, by integrating the equation of motion starting

[1] To be completely fair, the precise closed orbit is not known in synchrotrons in the region of the dipoles' fringing fields, except in the limiting case of hard-edged dipoles. But it's known well enough for most purposes.

at some radius and azimuth with an orbit that does not close, and then varying (r, P_r) in an iteration towards the periodic one using Newton's method. The transfer matrices, Twiss parameters can then be found along the orbit by using the same integration. The simplest approach is to use the polar coordinate azimuth θ rather than path length as the independent variable. This is the topic of the next chapter.

Chapter 3

Transverse Dynamics

In an accelerator, the particles are not only accelerated but we want them to remain "organized" in the sense of minimizing the phase space volume they occupy. From Liouville's theorem, we know that this volume is constant, but we also want the volume to be "simple" or simply-connected and the simplest way to do this is to ensure that the motion is linear. The idea of a periodic accelerator is that the particles access the same electric field turn after turn; this increases the efficiency over single-pass machines such as linear accelerators.

For any system of fields that returns particles to their starting point, there is at least single periodicity but generally the machine is divided into sectors that are intended to be identical. We know from the Floquet theorem or equivalently the Bloch theorem of electron orbits in solids, that there always exists an orbit that closes on itself and thus has the same symmetry as the field. But *a priori* in cyclotrons this closed orbit is not known. In synchrotrons by contrast, the orbit is known: in straight sections it is coaxial with quadrupoles, and in curved sections it is a circular arc of constant dipole field B and radius ρ whose product matches the particle's momentum per charge ($B\rho = p/q$). But in cyclotrons and other fixed field accelerators (FFAs), these conditions do not obtain: the magnetic field and its derivatives are everywhere spatially varying.

In linear channels and in synchrotrons, it is convenient to use the distance (s) along the reference orbit as the independent variable. Particles encounter fields and acceleration gaps at given s, not at given time, so this simplifies integration setup. In this system, time is another dependent variable. So a viable approach for cyclotrons is to guess at closed orbit coordinates at $s = 0$, and track the particle in the median plane using the known magnetic field (whether a design field or a measured one) on a grid of a chosen coordinate system. One could simply use the Lorentz force law for the equation of motion: $d\vec{p}/dt = q\vec{v}\times\vec{B}$ and adjust the starting coordinates until the orbit closes, call this the reference orbit, then find

the linear motion about it using the standard equations of the Frenet-Serret coordinate system[17].

But with cyclotrons, not knowing the reference orbit, it is most convenient to use the polar azimuth coordinate (θ) as independent variable. The main reason is that the magnetic field is measured usually using a survey device that pivots about the centre of the cyclotron magnet, taking measurements at set values of θ. The data are stored in an (r, θ) array, and when integrating, the θ increment can be used as Runge-Kutta step size. This greatly simplifies calculation of magnetic fields since the only interpolation needed is radial.

3.1 Equations of Motion

The basic equation containing the Hamiltonian and from which the equations of motion of charged particles in electromagnetic fields can be derived, is the following[18]:

$$(E - q\Phi)^2 - p^2c^2 = m^2c^4. \tag{3.1}$$

In Cartesian coordinates (t, x, y, z), canonical momenta are the 4 components (E, P_x, P_y, P_z), and the momentum components are related to the ordinary (kinetic) momentum components $\vec{p} = (p_x, p_y, p_z) = \gamma m\vec{v}$ as

$$p_x = P_x - qA_x \tag{3.2}$$
$$p_y = P_y - qA_y \tag{3.3}$$
$$p_z = P_z - qA_z \tag{3.4}$$

With time as independent variable, we solve 3.1 for E, insert the canonical momenta and that is our Hamiltonian $\mathcal{H} = E$.

$$\mathcal{H}_t(x, P_x, y, P_y, z, P_z) = E = q\Phi + c\sqrt{m^2c^2 + (P_x - qA_x)^2 + (P_y - qA_y)^2 + (P_z - qA_z)^2} \tag{3.5}$$

But with any other spatial coordinate as independent variable, the Hamiltonian is the negative momentum canonically conjugate to that spatial coordinate. For example, in the case of the Frenet-Serret coordinate system, the fundamental relation among the canonical variables is

$$\left(\frac{E - q\Phi}{c}\right)^2 = m^2c^2 + \frac{(P_s - qA_s)^2}{\left(1 + \frac{x}{\rho}\right)^2} + (P_x - qA_x)^2 + (P_z - qA_z)^2 \tag{3.6}$$

where $\rho = \rho(s)$ is the radius of curvature of the reference trajectory at location s.

The s-independent-variable Hamiltonian is

$$\mathcal{H}_s(x, P_x, z, P_z, t, E) = -P_s = -qA_s - \left(1 + \frac{x}{\rho}\right)\sqrt{\left(\frac{E - q\Phi}{c}\right)^2 - m^2c^2 - (P_x - qA_x)^2 - (P_z - qA_z)^2} \tag{3.7}$$

In polar coordinates (r, θ, z), the ordinary momentum consists of the components along these three directions (p_r, p_θ, p_z) but the corresponding canonical momenta (P_r, P_θ, P_z) are related to the ordinary ones as follows:

$$p_r = P_r - qA_r \tag{3.8}$$
$$p_\theta = P_\theta/r - qA_\theta \tag{3.9}$$
$$p_z = P_z - qA_z. \tag{3.10}$$

The Hamiltonian with θ as the independent variable is $\mathcal{H} = -P_\theta = -r(p_\theta + qA_\theta)$ and hence solving eqn. 3.1 for P_θ:

$$\mathcal{H} = -r(p^2 - p_r^2 - p_z^2)^{1/2} - q\,r\,A_\theta\ , \tag{3.11}$$

In this case the conjugate pairs are (r, P_r), (z, P_z), and (t, E). It is understood that (p_r, p_z) are replaced as in eqns. 3.8,3.10 before partial derivatives are taken to find the equations of motion. Additionally, we have defined p:

$$p^2 = \frac{1}{c^2}(E - q\,\Phi)^2 - m^2c^2 = (\gamma^2 - 1)m^2c^2 = 2mK\left(1 + \frac{K}{2mc^2}\right). \tag{3.12}$$

(K is the usual "kinetic" energy $(\gamma - 1)mc^2$.) Hamilton's canonical equations then lead to the following derivatives with respect to θ

$$r' = \frac{r\,p_r}{\sqrt{p^2 - p_r^2 - p_z^2}} \tag{3.13}$$
$$p_r' = \sqrt{p^2 - p_r^2 - p_z^2} + q(r\,B_z - z'\,B_\theta) + q\,t'\,\mathcal{E}_r \tag{3.14}$$
$$z' = \frac{r\,p_z}{\sqrt{p^2 - p_r^2 - p_z^2}} \tag{3.15}$$
$$p_z' = q(r'\,B_\theta - r\,B_r) + q\,t'\,\mathcal{E}_z \tag{3.16}$$
$$t' = \frac{\gamma\,m\,r}{\sqrt{p^2 - p_r^2 - p_z^2}} \tag{3.17}$$
$$E' = q(r'\,\mathcal{E}_r + r\,\mathcal{E}_\theta + z'\,\mathcal{E}_z) \tag{3.18}$$

where $\vec{B}$ is the magnetic field, and $\vec{\mathcal{E}}$ is the electric field.

Exercise: Derive these equations from the Hamiltonian. Note that Hamilton's equations give e.g. P_r', not p_r'. Example: $p_r' = P_r' - qA_r'$.

These are the exact equations of motion in cylindrical coordinates. It is worth noting that in the equations of motion, while z and p_z are small, first order quantities, r and p_r are not; they are zeroth order when the magnetic field varies with θ (i.e. is "AVF").

3.2 The magnetic field

For cyclotron applications, there is a flat median plane, at least in the design stage. This brings up the usual situation that there are two separate uses for such calculations: (1) In the design stage where fields are assumed to have correct symmetry, and (2) in the operation phase where the magnetic field is not the idealized desirable one, but the one that has been measured. The second case is also used in final design stages where tolerance against non-ideal field, misalignments, are to be estimated.

Gauge freedom allows us to choose the vertical component of $\vec{A}$ to be zero. Then $\vec{B} = \nabla \times \vec{A}$ gives:

$$B_r = -\frac{\partial A_\theta}{\partial z} \tag{3.19}$$

$$B_\theta = \frac{\partial A_r}{\partial z} \tag{3.20}$$

$$B_z = \frac{1}{r}\frac{\partial}{\partial r}(rA_\theta) - \frac{1}{r}\frac{\partial A_r}{\partial \theta} \tag{3.21}$$

But in general we have the magnetic field, not the vector potential. In fact, we have the magnetic field on the median plane, whether by a Laplace solver or by measurement. In that case, we can get the magnetic field in all space from the Maxwell equations.

The magnetic field can also be expressed in terms of a scalar potential Ψ:

$$\vec{B} = -\nabla\Psi; \quad \nabla^2\Psi = 0. \tag{3.22}$$

Under conditions of perfect median plane symmetry, Ψ has a closed form expression:

$$\Psi(r,\theta,z) = \sum_{n=0}^{\infty} \frac{(-)^n}{(2n+1)!}[\nabla_2^{2n} B(r,\theta)]z^{2n+1} \tag{3.23}$$

where ∇_2^{2n} is the 2-dimensional Laplacian, in polar coordinates given by

$$\nabla_2^2\Psi = \frac{1}{r}\frac{\partial}{\partial r}\left(r\frac{\partial\Psi}{\partial r}\right) + \frac{1}{r^2}\frac{\partial^2\Psi}{\partial\theta^2}, \tag{3.24}$$

applied n times. But it is almost always true that only the first term is needed. This is because the values of z needed for dynamics are the beam size and this is small compared to the magnet gap. The exceptions are investigations of nonlinear betatron resonances. Hence, we have simply $\Psi(r,\theta,z) = zB(r,\theta)$ and

$$\begin{aligned} B_r(r,\theta,z) &= -\frac{\partial\Psi}{\partial r} = -z\frac{\partial B}{\partial r} \\ B_\theta(r,\theta,z) &= -\frac{\partial\Psi}{r\partial\theta} = -\frac{z}{r}\frac{\partial B}{\partial\theta} \\ B_z(r,\theta,z) &= -\frac{\partial\Psi}{\partial z} = -B. \end{aligned}$$

3.2.1 Fields to Any Order: The Gordon Approach

This section is taken verbatim from the notes of Dr. Morton Gordon, a pioneer in cyclotron beam dynamics. The approach is typical of work going back to the MURA days in the 50s. Another more recent derivation, with the same results but much longer proof, can be found in a paper by Hart et al.[19].

In addition to $\nabla \cdot \vec{B} = 0$, we can take $\nabla \times \vec{B} = \vec{0}$ in the region occupied by the beam (neglecting the field produced by the beam itself). The $\vec{B}$ field can therefore be represented by either a scalar potential Ψ or a vector potential $\vec{A}$.

Scalar Potential

Since we are interested in orbits on or near the median plane $z = 0$, we expand the potential and, hence, the field in powers of z. Since $\nabla \times \vec{B} = \vec{0}$, we can set $\vec{B} = -\nabla\Psi$, and hence, since $\nabla \cdot \vec{B} = 0$ also, we have:

$$\nabla^2\Psi = \frac{\partial^2\Psi}{\partial z^2} + \nabla_2^2\Psi = 0, \tag{3.25}$$

where ∇_2^2 is the 2-dimensional Laplace operator (3.24). We can obtain a neat solution for Ψ in the form desired by an old trick from operator calculus. That is, in the above differential equation for Ψ we treat ∇_2 as if it were a constant. The 3-dimensional Laplace equation then looks like a simple oscillator equation. The general solution can therefore be taken as follows:

$$\Psi = \nabla_2^{-1}\sin(\nabla_2 z)B + \cos(\nabla_2 z)C, \tag{3.26}$$

where $B = B(r,\theta)$ and $C = C(r,\theta)$ are the two "constants"given by the "initial conditions" at $z = 0$. I.e. for $z \to 0$, $\Psi \to C$, and $\frac{\partial\Psi}{\partial z} \to B$. This solution then holds for arbitrary z.

It is understood, of course, that B and C are actually operands, and that $\sin(\nabla_2 z)$ and $\cos(\nabla_2 z)$ must be replaced by their power series when performing explicit calculations. Thus, if we write $\Psi = \Psi_\mathrm{o} + \Psi_\mathrm{e}$, then the odd and even parts of Ψ are given by:

$$\Psi_\mathrm{o} = zB - \frac{z^3}{3!}\nabla_2^2 B + \frac{z^5}{5!}\nabla_2^4 B - ..., \tag{3.27}$$

and

$$\Psi_\mathrm{e} = C - \frac{z^2}{2!}\nabla_2^2 C + \frac{z^4}{4!}\nabla_2^4 C - ... \tag{3.28}$$

Note that Ψ_o produces a field with perfect median plane symmetry, while Ψ_e spoils this symmetry.

Note also that $B_z = -\partial\Psi/\partial z$ is given in general by:

$$B_z = -\cos(\nabla_2 z)B + \sin(\nabla_2 z)\nabla_2 C, \tag{3.29}$$

and this B_z is also a general solution of the 3-dimensional Laplace equation. Since the part generated by C corresponds to an "error field", we take $C = 0$ in this simplified treatment

$$B_z = -B + \frac{z^2}{2!}\nabla_2^2 B - \frac{z^4}{4!}\nabla_2^4 B + ... \tag{3.30}$$

while the corresponding expressions for B_r and B_θ are:

$$B_r = -z\frac{\partial B}{\partial r} + \frac{z^3}{3!}\frac{\partial \nabla_2^2 B}{\partial r} - ... \tag{3.31}$$

$$B_\theta = -\frac{z}{r}\frac{\partial B}{\partial \theta} + \frac{z^3}{3!r}\frac{\partial \nabla_2^2 B}{\partial \theta} - ... \tag{3.32}$$

Thus, the entire field off the median plane can be expressed in terms of B and its derivatives.

In most orbit programs, we use only the zero order B_z value and the first order values of B_r and B_θ. This is acceptable only for z small compared with the magnet gap since it violates $\nabla \cdot \vec{B} = 0$ and can therefore lead to non-physical results for finite z values. This can be remedied by including the z^2 term in B_z. In general, when B_r and B_θ are given to order z^n, then B_z should be given to order z^{n+1}.

Vector Potential

The vector potential is required to form the Lagrangian or Hamiltonian. Here, $\vec{A}$ is entirely defined by $\vec{B} = \nabla \times \vec{A}$ and therefore requires $\nabla \cdot \vec{B} = 0$.

Note that $\vec{A}$ is far from unique since for an arbitrary spatial function f, we can use $\vec{A} + \nabla f$ just as well (gauge invariance). We use this freedom to set $A_z = 0$ and then determine A_r and A_θ to reproduce the given $\vec{B}$.

With $A_z = 0$, the components of $\vec{B} = \nabla \times \vec{A}$ are given by:

$$B_r = -\frac{\partial A_\theta}{\partial z},\ B_\theta = +\frac{\partial A_r}{\partial z} \tag{3.33}$$

$$B_z = \frac{1}{r}\frac{\partial}{\partial r}(rA_\theta) - \frac{1}{r}\frac{\partial A_r}{\partial \theta}. \tag{3.34}$$

Now, for $z = 0$, $B_z = -B$ and $B_r = B_\theta = 0$ (neglecting imperfections). In this case, $A_r \to 0$ and:

$$A_\theta \to -\frac{1}{r}\int rB(r,\theta)dr. \tag{3.35}$$

For vaues off the median plane, we can use the power series for the $\vec{B}$ components found above. Hence, we can write:

$$A_r = \int B_\theta dz, \tag{3.36}$$

$$A_\theta = -\frac{1}{r}\int rBdr - \int B_r dz, \tag{3.37}$$

and since B_r and B_θ contain only odd powers of z, it follows that $\vec{A}$ contains only even powers (i.e., odd z terms in $\vec{A}$ result from error fields).

Since $\vec{B} = -\nabla\Psi$, we can also write:

$$A_r = -\frac{1}{r}\frac{\partial}{\partial\theta}\left(\int \Psi dz\right), \tag{3.38}$$

$$A_\theta = -\frac{1}{r}\int rBdr + \frac{\partial}{\partial r}\left(\int \Psi dz\right), \tag{3.39}$$

with:

$$\int \Psi dz = \frac{z^2}{2}B - \frac{z^4}{4!}\nabla_2^2 B + ... \tag{3.40}$$

Exercise: Verify that this gives the correct B_z as well as B_r and B_θ.

Note that keeping terms in A_r and A_θ to order z^{2n} gives B_z to this order, but B_r and B_θ only to order z^{2n-1} as required for $\nabla\cdot\vec{B} = 0$. Note also that $\nabla\times\vec{B} \neq \vec{0}$, which corresponds to a current density $\vec{J} \sim z^{2n}$.

3.3 Finding the closed orbit

The closed orbit is for the case of no electric field, no acceleration, E=constant.

Does a closed orbit always exist? Yes, if it is bounded. This follows from Floquet theory, and is analogous to the Bloch theorem of solid state physics to describe electron orbits in a crystalline lattice. In any periodic potential, a closed orbit exists for a given energy if the motion is bounded[1]. Of course if the energy is out of the range of the cyclotron, the orbit will not be bounded, or will intersect the magnet steel or coils. An interesting fact about closed orbits, first proved by Courant & Snyder [17, Appendix A] is that the amount of flux enclosed by the closed orbit is a maximum. This follows from Hamilton's principal.

[1]It can happen that the motion is not bounded. This would be an intrinsic betatron resonance for a limited energy range, and is analogous to a band gap for electrons in condensed matter physics.

Under conditions of a flat median plane, it is clear that $z = p_z = 0$ is a particular solution: particles in the median plane stay in the median plane. Thus we look for closed orbits in the median plane. The equations then become:

$$r' = \frac{r\,p_r}{\sqrt{p^2 - p_r^2}} \tag{3.41}$$

$$p_r' = \sqrt{p^2 - p_r^2} + qr\,B_z \tag{3.42}$$

$$t' = \frac{\gamma\,m\,r}{\sqrt{p^2 - p_r^2}} \tag{3.43}$$

Exercise: Use these equations to show the expected behaviour for (1) Flat field B=constant independent of (r, θ) and $p_r \ll p$, and (2) Exact solution for $B = 0$ (hint: try a substitution $p_r = p \sin\psi$.)

We proceed as Gordon[20, 21]. The notation is now simplified if we use the substitution

$$p_\theta = \sqrt{p^2 - p_r^2}. \tag{3.44}$$

We would like the equations of small oscillations of r and p_r so we substitute

$$r \to r + x, \quad p_r \to p_r + p_x \tag{3.45}$$

and then expand the equations to first order in x and p_x. An equivalent but more elegant technique is to make the substitution 3.45 into a canonical transformation to find a new Hamiltonian that contains only (x, p_x) which are first order perturbations about the periodic particular solution (r, p_r).

When this is done, we find

$$x' = \frac{p_r}{p_\theta}x + \frac{rp^2}{p_\theta^3}p_x \tag{3.46}$$

$$p_x' = -q\left[B + r\frac{\partial B}{\partial r}\right]x - \frac{p_r}{p_\theta}p_x, \tag{3.47}$$

where r and p_r have the same values at each θ as those used on the right side of Eqs. 3.41, 3.42 during the integration.

In order to generate the basic transfer matrix, we need two independent solutions of these equations, and these are denoted as $(x_1(\theta), p_{x1}(\theta))$ and $(x_2(\theta), p_{x2}(\theta))$. We are free to choose any initial ($\theta = 0$) conditions $(x(0), p_x(0))$, and the most convenient is to choose $(x_1(0), p_{x1}(0)) := (1, 0)$ and $(x_2(0), p_{x2}(0)) := (0, 1)$, for then the final values ($\theta = \theta_\mathrm{f} := 2\pi/N$) after integration through one period (one sector) are the elements of the transfer matrix:

$$M_x := \begin{pmatrix} x_1(\theta_\mathrm{f}) & x_2(\theta_\mathrm{f}) \\ p_{x1}(\theta_\mathrm{f}) & p_{x2}(\theta_\mathrm{f}) \end{pmatrix} \tag{3.48}$$

We note in passing that this technique of finding the general solution for the evolution of the *differential* coordinate pair (x, p_x) is simply a restricted case of the DA approach used in COSY-∞[22], though without the *automatic differentiation* for deriving the equations 3.46, 3.47.

In cyclotron orbit codes, integration of all five equations 3.41, 3.42, 3.43, 3.46, 3.47 is performed simultaneously, at the end of which we have orbit coordinates $(r(\theta_\mathrm{f}), p_r(\theta_\mathrm{f}))$ and the transfer matrix. To find the closed orbit we apply the inverse of the transfer matrix to the difference $(\epsilon_r, \epsilon_p) = (r(\theta_\mathrm{f}) - r(0), p_r(\theta_\mathrm{f}) - p_r(0))$. Explicitly, if the closed orbit at $\theta = 0$ and $\theta = \theta_\mathrm{f}$ is denoted $(r_\mathrm{c}, p_\mathrm{rc})$, the expected behaviour is

$$\begin{pmatrix} r_\mathrm{c} \\ p_\mathrm{rc} \end{pmatrix} = \begin{pmatrix} r(\theta_\mathrm{f}) \\ p_r(\theta_\mathrm{f}) \end{pmatrix} + M_x \left[\begin{pmatrix} r_\mathrm{c} \\ p_\mathrm{rc} \end{pmatrix} - \begin{pmatrix} r(0) \\ p_r(0) \end{pmatrix} \right]. \tag{3.49}$$

Solving for the closed orbit, we get:

$$r_\mathrm{c} = r(0) + \frac{(M_{22} - 1)\epsilon_r - M_{12}\epsilon_p}{M_{11} + M_{22} - 2} \tag{3.50}$$

$$p_\mathrm{rc} = p_r(0) + \frac{(M_{11} - 1)\epsilon_p - M_{21}\epsilon_r}{M_{11} + M_{22} - 2} \tag{3.51}$$

If linear, this is exact, but if not, we simply repeat the process. This has the same convergence property as Newton's method: precision squares at every iteration. Usually, no more than two or three iterations are needed to reach single precision ($\sim 10^{-7}$) limit.

The same linearization can be repeated for the vertical motion:

$$z' = \frac{r}{p_\theta} p_z \tag{3.52}$$

$$p_z' = q \left[r \frac{\partial B}{\partial r} - \frac{p_r}{p_\theta} \frac{\partial B}{\partial \theta} \right] z \tag{3.53}$$

and these integrated to find the vertical orbit properties once the closed orbit is known, or simultaneously with the other five ODEs.

3.4 Courant-Snyder parameters

Once found, the integration has produced not only the closed orbit, but also the transfer matrix $M(\theta)$ that takes one from starting point to θ, from $M(\theta_\mathrm{f})$ the tune ν (whether ν_x or ν_z) can be found from the arccosine of the half-trace:

$$\cos \nu\theta_\mathrm{f} = \frac{1}{2}(M_{11} + M_{22}) \tag{3.54}$$

The Courant-Snyder parameters as a function of θ can also be found from the transfer matrix as a function of θ. This is a standard procedure used in synchrotron codes such as `MAD`, `DIMAD`, `SAD`, `SYNCH`, etc. Briefly, we have the matrix $M(\theta)$ which takes the coordinates from the starting point ($\theta = 0$) to some azimuth θ. We want the periodic matrix $M_{\rm p}(\theta)$ which takes the coordinates from θ to $\theta + \theta_{\rm f}$. The missing piece is the matrix that takes one from θ to $\theta_{\rm f}$. This is clearly $M(\theta_{\rm f})M^{-1}(\theta)$. (Remember: right to left, first backtrack to zero, then forward-track through the complete sector.) Then we forward-track a further distance of θ, finally giving:

$$M_{\rm p}(\theta) = M(\theta)M(\theta_{\rm f})M^{-1}(\theta) \tag{3.55}$$

Courant-Snyder parameters $\alpha(\theta), \beta(\theta), \gamma(\theta)$ are then found by equating:

$$M_{\rm p}(\theta) = \begin{pmatrix} \cos\mu + \alpha\sin\mu & \beta\sin\mu \\ -\gamma\sin\mu & \cos\mu - \alpha\sin\mu \end{pmatrix} \tag{3.56}$$

where μ is the phase advance per period, $\nu\theta_{\rm f}$. The matrices can be expanded to give the usual C-S parameter evolution matrix:

$$\begin{pmatrix} \beta \\ \alpha \\ \gamma \end{pmatrix} = \begin{pmatrix} M_{11}^2 & -2M_{11}M_{12} & M_{12}^2 \\ -M_{11}M_{21} & M_{11}M_{22} + M_{12}M_{21} & -M_{12}M_{22} \\ M_{21}^2 & -2M_{21}M_{22} & M_{22}^2 \end{pmatrix} \begin{pmatrix} \beta_0 \\ \alpha_0 \\ \gamma_0 \end{pmatrix} \tag{3.57}$$

Note the similarity transformation preserves the trace when $\det[M(\theta)] = 1$ i.e. M is symplectic, as it must be. This determinant can be used to check the precision of the numerical Runge-Kutta integration.

Once past the design stage and into commissioning, and further for modelling the cyclotron during operation, the axially symmetric and perfectly periodic field is replaced by measurement results. Even in the design stage, it may be advisable to insert random section and symmetry errors into the design field to investigate stability against such errors. In these cases, the only periodicity is a full turn, and the field components B_r and B_θ are non-zero on the mid-plane. For small cyclotrons, the effects of these errors can be approximated analytically, but for large cyclotrons like TRIUMF, this is not the case. Having non-zero B_r and B_θ at $z = 0$ results in the closed orbit not being in the mid-plane, so the orbit code has to be expanded to allow this. This was done at TRIUMF[23]. The technique is exactly the same as described above for the radial motion: The linearized vertical motion equations (3.52, 3.53) are used to find the transfer matrix and this is used to iterate toward the closed orbit. An interesting complication arises because the vertical closed orbit depends upon derivatives of the magnetic field. The field values must be accurate, and if the radial interpolation is not perfomed well, these derivatives will be discontinuous, making convergence difficult and the tune inaccurate[24].

A further complication of analyzing a full turn is that the betatron phase advance is then larger than π. The equation 3.54 can then not provide the integer part of the tune. One

way to find it is to simply count the number of sign reversals of the trace. For example, the TRIUMF cyclotron has six sectors and the radial tune is greater than 1.5 (phase advance exceeds 3π). A robust algorithm to find the tune is given by Colleen Meade[25].

Chapter 4

Longitudinal Dynamics

4.1 The "Accelerated Equilibrium Orbit"

It may not be obvious, but accelerated particles in a cyclotron do not automatically "spiral outward" or maintain otherwise a small distance from the equilibrium orbit of the particle's particular energy. Intuitively we expect that if the closed orbit radius gain per turn is a small fraction of the radius, then all particles will remain near the closed orbit corresponding to their particular energy. But there can be resonance effects. An extreme example would be a radial tune of 1, and a single energy gain per turn. In that case, the particle orbits continue to pass through the cavity even though the orbit radius continues to grow, as in Fig. 4.1; it will act as a microtron.

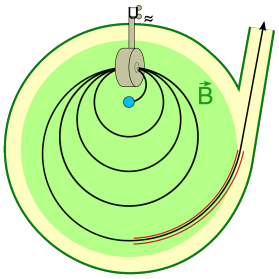

Figure 4.1: Microtron orbits.

The situation can be compared with "synchro-betatron" effects in synchrotrons. If acceleration cavities are in locations of dispersion (as they always are in cyclotrons), the reference orbit displaces horizontally as a particle passes through. These displacements can accumulate or not depending on the phase relationship between horizontal and longitudinal motions; they accumulate if the transverse tune lies on a synchrotron sideband of the integer. But in the case of cyclotrons, the synchrotron tune is zero, so the resonance is directly on the integer.

For simplicity, we assume energy kicks to be at the short limit (δ-functions). These kicks need not be all equally separated in orbit angle, but again for simplicity and pedagogical purposes, we assume this to be the case. Between these kicks, the particles simply execute betatron oscillations, and at each kick, the equilibrium orbit, about which the betatron oscillations occur, increments to the new orbit for the new energy. The combination of

these two motions is shown in the case of two kicks per turn, $\nu_r \sim 1.3$, in Fig. 4.2. The motion of the particles is made optimally smooth by proper choice of betatron amplitude for the reference particle. The trajectory it then follows is called the "accelerated equilibrium orbit".

Let θ_D be the orbit angle between rf gap crossings. Then the betatron amplitude r_{AEO} condition for a smooth AEO can be found by simple trigonometry:

$$r_{\mathrm{AEO}} = \frac{\delta r}{2\sin(\nu_r \theta_D/2)} \tag{4.1}$$

$\delta r = \frac{R_\infty}{\beta\gamma^3}\frac{\delta E}{mc^2}$ is the average, intended radius gain per rf gap crossing commensurate with the energy gain δE per crossing.

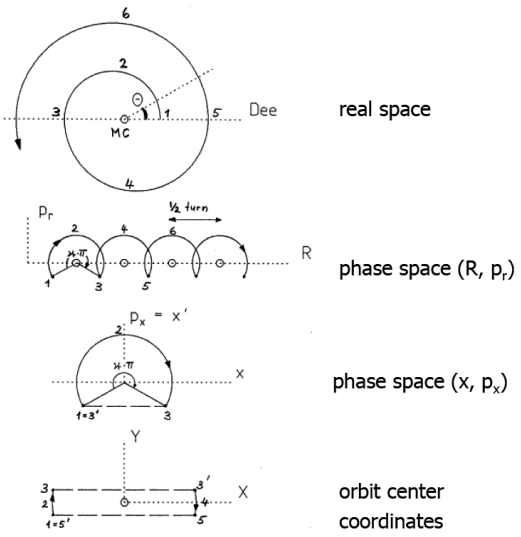

Figure 4.2: Accelerated orbits (Joho, 2011[26]).

Check: (1) If $\nu_r\theta_D = 2\pi$, there is no solution as the orbit moves continuously away from the equlibrium orbit, as discussed for microtrons above. (2) In the limit of $\nu_r\theta_D \ll 1$, the orbit converges to a constant displacement in the p_r direction of $\delta r/(\nu_r\theta_D)$. This p_r represents the angle of outward spiral, as in this limit, the particles spiral smoothly outward. Keep in mind that as θ_D diminishes, δr does too, if one is to maintain energy gain per turn: $\delta r = \Delta r\frac{\theta_D}{2\pi}$ where Δr is radius gain per turn, so $r_{\mathrm{AEO}} = \frac{\Delta r}{2\pi\nu_r}$. This angle is found by dividing by the average radius of the orbit, so for $\nu_r = 1$ we find as expected the angle $\frac{dr}{ds} = \frac{\Delta r}{2\pi r}$.

Shown below (Fig. 4.3) is the TRIUMF cyclotron centre post, injection scheme and first four turns. Particles come through the inflector and then the "deflector" with an energy of precisely 300 keV. At the first gap, the particle on crest gains energy 100 keV, and at each of the subsequent gaps gains 200 keV. The radial tune, $\nu_r = 1$. This technique where the injection acceleration gap is at the same azimuth as the other gaps but has half the voltage of the subsequent ones, was an innovation by G. Dutto[27]. Its advantage is that it minimizes injection errors for all rf phases of accepted particles.

Exercise: For the TRIUMF case as in Fig. 4.3, what is the correct radius, at the first gap, that the beam should be injected assuming the magnetic field is 0.3T and the particle is H^-? Show by making a diagram as in Fig. 4.2 why this scheme of having the first gap at half the energy gain of subsequent ones results in perfectly centred orbits independent of their phase with respect to the rf. Indicate on the plot the effect of varying the voltage on the "deflector".

This is not of course a general case. In general, both r and p_r are functions of energy as well as θ. And in general, there are not two dee gaps, but typically there are separate rf cavities for acceleration, and the rf frequency is an integer multiple of the revolution frequency. The acceleration gaps have to be arranged, as in a linear accelerator, so that their overall effect is to accelerate efficiently. At the initial stage, the rf system can be designed using the type of geometrical argument given above for the two dee-gaps-per-turn case. The general case can be more deeply understood by investigating the Hamiltonian including the rf fields.

Ring cyclotrons are those whose injection energy is sufficiently high that no magnetic field is required at $R = 0$. If such a cyclotron has separated sectors, rf cavities can be placed between the sectors. These are similar to a synchrotron arrangement, but with the orbits and therefore the cavities extended in the radial direction (as in Fig. 2.6). Each cavity provides a single accelerating gap to the beam and each can be phased appropriately. This frees the choice of harmonic number h and is an efficient way to obtain large voltage per turn. By contrast, small cyclotrons tend to have electrodes that act as drift chambers, as in a DTL. The electrode is excited by a quarter-wave resonator, and the harmonic number must be such that the rf phase changes sign as the particles in a bunch travel from the entrance gap to the exit. If the change is 180°, they obtain a maximal acceleration at both the entrance and the exit. When the electrodes are themselves 180°, any harmonic number is possible (and in this case, it's obvious why they are called "dees"), but in general the dee is wedge-shaped to fit into the magnetic field "valley" between two sectors. Thus if there are 4 sectors, each 45° wide, the dees themselves are also 45°, and the rf must have a frequency of $h = 180/45 = 4$ times the revolution frequency, or any multiple of 4, to obtain maximal acceleration efficiency.

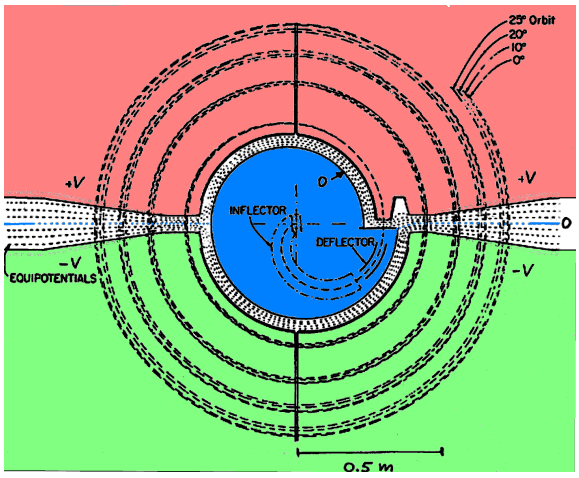

Figure 4.3: Centre region of the TRIUMF cyclotron. The dees are coloured: red and green. The centre post is at ground (blue). The dashed lines are four orbits with phases as indicated; 0° is "on-crest". The dotted lines are equipotentials.

The particles rotate as the spokes of a wheel, there are h spokes, each occupying an angular width according to the phase width (ϕ) of the particles: $\Delta\theta = \Delta\phi/h$ where h is the harmonic number. For perfectly isochronous motion, this phase width is a constant i.e. the spokes have a constant angular width. But there are two effects that change this picture: non-constant accelerating voltage, and space charge, covered later in this text. If there are isochronism errors, the spokes are not radially straight.

4.2 Isochronism errors

Recall the "longitudinal" coordinates (t, E), eqns. 3.17, 3.18. The first of these is simply $rd\theta/dt = v_\theta$ (recall that $p_\theta = \sqrt{p^2 - p_r^2 - p_z^2}$) written as a reciprocal:

$$\frac{dt}{d\theta} = \frac{r}{v_\theta} =: \frac{1}{\omega}. \tag{4.2}$$

The "beam frequency" ω thus defined is a function of E, and is found in the orbit code when eqn. 3.17 is integrated as the equilibrium orbit is found. If it's a sufficiently slow function of E, integrate to find $\omega(E)t - \theta =$ constant. The idea of course is to design the magnetic field such that this frequency is a constant to some precision and accelerate at a multiple (h) of this frequency: $\omega \approx \omega_{\rm rf}/h$. But what precision is needed?

The change in energy due to the acceleration rf field is calculated in orbit codes as in equation 3.18. This can be identified as simply:

$$\frac{dE}{d\theta} = q\vec{\mathcal{E}} \cdot \frac{d\vec{s}}{d\theta} \tag{4.3}$$

For the moment we assume the electric field is parallel to the equilibrium orbit and located at gaps θ_j.

$$\mathcal{E}_j(\theta, t) = \frac{\delta_{\rm p}(\theta - \theta_j)}{R} V_j \cos(\omega_{\rm rf} t + \phi_{0j}) = \\ \frac{V_j}{4\pi R} \sum_{n=-\infty}^{\infty} \exp[i(n\theta + \omega_{\rm rf} t + \phi_{0j} - n\theta_j)] + \exp[i(n\theta - \omega_{\rm rf} t - \phi_{0j} - n\theta_j)] \tag{4.4}$$

(The function $\delta_{\rm p}(\theta)$ is a periodic δ-function with unity integral over one turn, and Fourier expanded here.) Only in the case of $n = \pm h$ is there a net acceleration over multiple turns, so we keep only those terms and thus:

$$\mathcal{E}_j(\theta, t) = \frac{V_j}{2\pi R} \cos(\omega_{\rm rf} t - h(\theta - \theta_j) + \phi_{0j}) \tag{4.5}$$

To recap: θ_j is the location of gap j, and ϕ_{0j} is the phase of this cavity. Acceleration occurs if the argument of the cosine for any j, is a constant, or near constant.

Over many turns, the detailed effect of individual gap crossings is unimportant (except in cases where the periodicity of gap crossings resonates with betatron motion), and we are interested in the cumulative effect, which is the same whether the voltage per turn is distributed over many gaps or just one. So we drop the sum over gaps. For maximum energy gain we want the argument of the cosine to be (close to) zero. Let us call this

argument ϕ, then $\phi = \omega_{\rm rf} t - h(\theta - \theta_0) + \phi_0$. We do not know yet how ϕ evolves, but we do know the derivative:

$$\frac{d\phi}{d\theta} = \omega_{\rm rf}\frac{dt}{d\theta} - h = \left(\frac{\omega_{\rm rf}}{\omega(E)} - h\right). \tag{4.6}$$

We substitute eqn. 4.5 into 4.3 to get the conjugate rate equation:

$$\frac{dE}{d\theta} = \frac{qV}{2\pi}\cos\phi \tag{4.7}$$

One can contruct the Hamiltonian from this pair of equations.

$$H(E,\phi;\theta) = \frac{qV}{2\pi}\sin\phi - \int\left(\frac{\omega_{\rm rf}}{\omega(E)} - h\right)dE \tag{4.8}$$

It may seem a facile way to obtain a Hamiltonian, but the interested reader is referred to the more rigorous derivation by Gordon[28]; we give here a brief description of his approach. From the Hamiltonian 3.11 the equilibrium orbits are found as a function of energy: $r := R(E,\theta)$, $p_r := P(E,\theta)$. A transformation is made where the new radial coordinates (x, p_x) are with respect to these: $r = x + R(E,\theta)$, $p_r = p_x + P(E,\theta)$. To keep it canonical, this necessitates a transformation of the time coordinate as well. Time is then scaled with angular position subtracted, to become the phase ϕ introduced above. (This is similar to the perhaps more familiar transformation used in synchrotrons to decouple the betatron motion from the longitudinal[29, 16]: $x \to x + D\Delta p/p$, $p_x \to p_x + D'\Delta p$, $\phi \to \phi - \frac{h}{R}(D\frac{p_x}{p_0} - D'x)$.) The physical reason is that in contrast to zero amplitude particles, particles with finite betatron amplitude take longer or shorter paths reaching a given location θ.

As H of eqn. 4.8 has no explicit dependence on the independent variable, it is a constant of motion. It follows that we can find the final phase of a particle knowing its initial phase $\phi_{\rm i}$ and the isochronism error as a function of E:

$$\sin\phi - \sin\phi_{\rm i} = \frac{2\pi}{qV}\int_{E_{\rm i}}^{E}\left(\frac{\omega_{\rm rf}}{\omega(E)} - h\right)dE \tag{4.9}$$

Knowing $\omega(E)$, the orbit frequency as a function of energy, and the rf voltage per turn V, we can plot phase histories in the longitudinal phase plane. Two examples are shown below: the TRIUMF 520 MeV cyclotron, and a hypothetical "EMMA"-like FFA with parabolic isochronism error[30]. In the TRIUMF case, the experimentally-measured phase history of the bunch average phase is plotted overlaid on the theoretical contours. The measurement was made during commissioning in 1975[31]. Note that these contours depend on V. There are islands centred on the crossover phase of 90°. (Note that we use the cyclotron convention where "on-crest" is zero degrees.) As the voltage per turn V is lowered, these islands expand laterally, at some point (the "pinch-off"), one of the extrema of the orbital

periods' oscillations will result in $\sin\phi > 1$, preventing further acceleration. Note that with any cyclotron, the field will eventually fall with radius, losing isochronism and causing particles to run over the zero degree phase and begin to decelerate. This establishes the maximum energy of that cyclotron. It was this phenomenon that allowed the measurement shown in Fig. 4.4. Without any extraction, there will be at any radius two bunches, one accelerating and the other decelerating, and their phase difference easily measured.

The integrand in eqn. 4.9 is basically the fractional frequency error. Besides the isochronism oscillations caused by the magnetic field, such an error can also be caused by either the rf frequency or the revolution frequency error due to magnetic field excitation error. If the fractional error is ϵ, $\sin\phi$ will slip by $2\pi h\epsilon\Delta E/(qV) = 2\pi h\epsilon n$ where n is the number of turns of the on-crest particle. If this is 1, the acceleration will stall; if larger than 1, the phase slip will pass 90° and the particles decelerate and return to the point of injection.

For the case of the TRIUMF cyclotron, there are 1400 turns to reach 500 MeV, and $h = 5$. This requires $\epsilon < 1/44,000$ or 23 parts per million. But this is for the best particle. Generally the phase acceptance desired for maximum intensity operation is 60° such that particles out to phases ±30° need to be included. This hardens the requirement by a factor two to 11 ppm. In fact, the magnetic field is not perfectly isochronous and there are phase excursions of a further ±30° or so (see Fig. 4.4), and this reduces the tolerance by a further factor of two. This "few ppm" error tolerance applies to both the rf frequency and the current supplied to the magnetic field coils. Either of these errors cause a monotonic deviation of the bunch's phase. With reference to the figures, this causes the contours to angle towards the right or left as the particles gain energy; see Fig. 4.6

Exercise: Use 4.9 to plot longitudinal phase space contours for a cyclotron with a parabolic fractional isochronism error. The result should be as shown in Fig. 4.5. This is basically the case for FFA's of the EMMA type[30]. Investigate the effect of varying the voltage per turn.

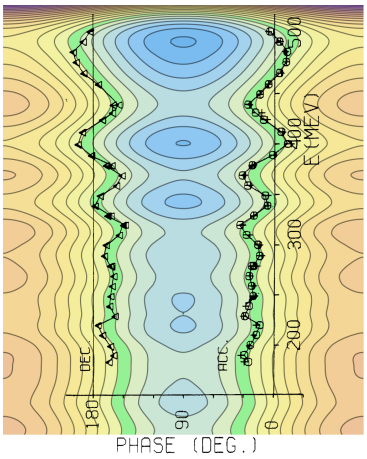

Figure 4.4: Black data points: Commissioning results from TRIUMF cyclotron, taken from [31]. Beam is allowed to accelerate through the region that is higher than the designed top energy, where the magnetic field falls off and is no longer isochronous, causing the beam to decelerate back towards the cyclotron's centre. A thin stripper foil extracts both the accelerated and decelerated beams and their time with respect to the rf reference is measured as the stripper is moved through the energy range. These data have been overlaid on the calculation from eqn. 4.9. The integral of the isochronism error was calculated (using the code `CYCLOP`) from magnetic field survey data taken in 1973. The closest match contour area is coloured green. The comparison is not expected to be exact, as there are 54 trim coils that are adjusted to fine-tune the isochronism.

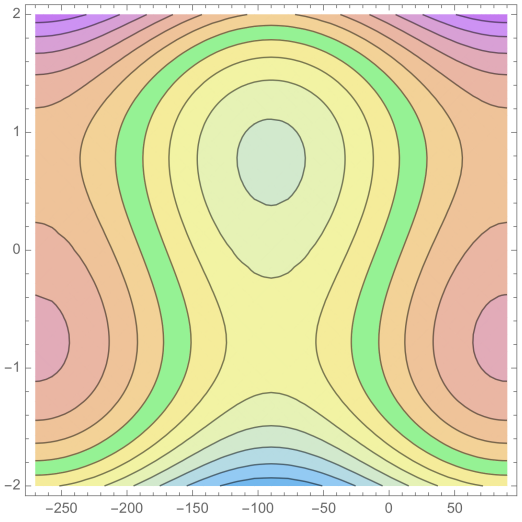

Figure 4.5: Phase space contours for a cyclotron with parabolic isochronism error. The horizontal axis is phase in degrees, and the vertical is energy difference with respect to some reference. The most efficient acceleration path is coloured green.

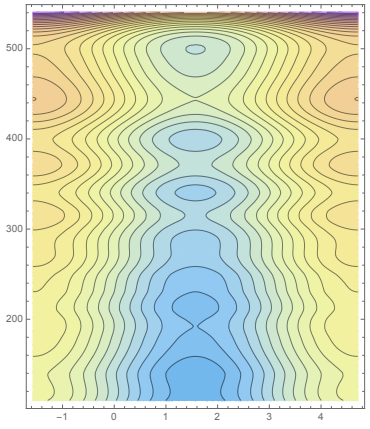

Figure 4.6: The TRIUMF case, plotted now with an rf frequency error of 40 ppm. Note that a particle starting on crest will not make it past 360 MeV.

4.3 Spatially-varying dee voltage

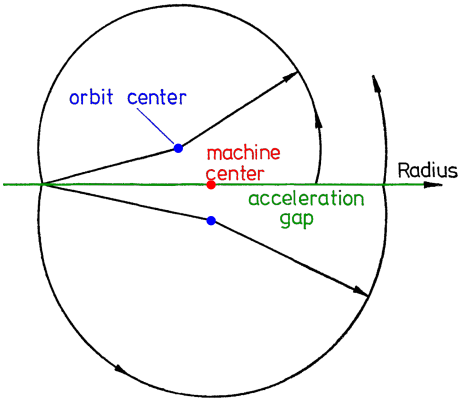

Figure 4.7: Orbits affected by non-constant accelerating field (Joho, 2011[26]).

Imagine a circulating particle bunch of finite phase width and energy width. As particles that differ in energy have differing average radius, the energy spread is reflected in the radial width of the bunch. If the energy gain per turn falls with radius, the energy spread will naturally fall as well, compressing the bunches radially. In other words, the outer particles will turn after turn receive less energy gain than the central particle, and the inner particles will continually receive more energy gain. By Liouville's theorem, since energy and time (phase in a constant frequency machine) are conjugate, we expect that when energy spread decreases, phase width increases. What is the origin of this phase width increase? Surprisingly, it is the rf **magnetic** field.

If the rf electric field, in the θ direction across the accelerating gap, is falling with r, then by $\nabla \times \vec{\mathcal{E}} = -\partial \vec{B}/\partial t$ there must be a vertical rf magnetic field at that location and as the Fig. 4.7 shows, this has the effect of kicking the orbits radially. The result with a falling gap voltage is that late particles take a longer path and arrive later still; early particles take a shorter path and arrive earlier still. This broadens the phase width of the bunch. Conversely, a rising voltage with radius shortens bunches and increases energy spread.

The effect is neatly described by the Hamiltonian 4.8. Leaving off the isochronous field or frequency error, the Hamiltonian is simply

$$H(E,\phi) = \frac{qV}{2\pi}\sin\phi \tag{4.10}$$

and because of the canonical transformation mentioned above, it remains valid even if the energy gain qV is a function of E through $R(E,\theta)$!

$$\frac{d\phi}{d\theta} = -\frac{\partial H}{\partial E} = -q\frac{\sin\phi}{2\pi}\frac{dV}{dE} \tag{4.11}$$

$$\frac{dE}{d\theta} = \frac{\partial H}{\partial \phi} = \frac{qV}{2\pi}\cos\phi \tag{4.12}$$

where $\frac{dV}{dE} = \frac{dV}{dR}\frac{\partial R}{\partial E}$, the dispersion $\frac{\partial R}{\partial E}$ being evaluated at the acceleration gap.

Again, since H does not explicitly depend upon θ, $V\sin\phi$ is an invariant. For example, if the initial extreme-phase particle in a cyclotron is ϕ_i, and the energy gain per turn varies

from qV_i at injection to qV_f at extraction, then that particle's final phase is given by

$$\sin\phi_\mathrm{f} = \sin\phi_\mathrm{i}\frac{V_\mathrm{i}}{V_\mathrm{f}}. \tag{4.13}$$

An explanation of this "phase compression effect" was first given by Joho[32] and later by Gordon in the paper already mentioned[28]. Gordon[33] christened the H above as the SSJ invariant because Joho's work had been preceded by Symon and Sessler in a paper entitled *Methods of Radio Frequency Acceleration in Fixed Field Accelerators with Applications to High Current and Intersecting Beam Accelerators*[34]. This paper expanded the concept of FFAGs by proposing beam stacking, a technique that was first realized in the Intersecting Storage Rings at CERN in 1974. It was also the first paper that showed the longitudinal phase space for parabolic isochronism error (compare Fig. 4.5 with their Fig. 7), and so can be said to have spawned storage rings, FFAGs, and high energy cyclotrons.

4.4 Non-radial RF gaps

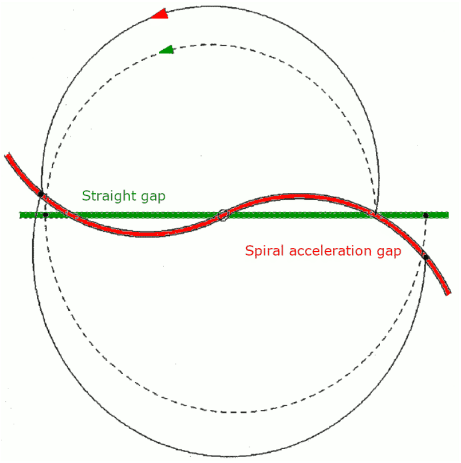

Figure 4.8: Spiral accelerating gap, intended to change particles' phase with respect to the RF, but does not. (Joho, 2011[26]).

In the 1970's, as superconducting-coil separated-spiral-sector cyclotrons with dee gaps lying between the sectors were being designed, a question arose as to whether an angled accelerating gap has any effect on the isochronism. Remarkably, it has no effect; the orbit period in a cyclotron is insensitive to the angle of the accelerating gap. This was first proved by Edwin McMillan in the 1950's who apparently kept no record of it. Gordon gives a concise explanation[35], and in a separate work, gives further a completely canonical proof as well [28].

A rough description is as follows. Consider a particle spiralling outward as it accelerates. Imagine the accelerating gaps spiral towards the particle so that the orbit period would naïvely be shortened, see Fig. 4.8. In order for this to be true, though, the angle of the gaps must be such as to give the particle an outward kick at each gap. This kick causes the particle to take a longer path thus increasing the orbit period. So the two effects are in opposition and surprisingly, they cancel **exactly** in first order.

As mentioned in section 2.2.2, a cyclotron with no sector focusing (a 'classical' cyclotron) requires the magnetic field to decrease with radius or else there is vertical defocusing. But isochronism requires a flat field or even an increasing one as relativistic effects begin. One could have the clever idea of compensating the decrease in revolution frequency with accelerating gaps which spiral towards the oncoming particles. This has been patented as recently as 2012[1]! But sadly there is no effect on isochronism, so the patent has no more merit than one for perpetual motion.

4.5 Longitudinal Optics And Extraction

In ordinary extraction such as single turn in a cyclotron, or in a synchrotron, the emittance is extracted wholesale. Particles injected into a cyclotron with equal energy but different phase follow neighbouring paths in E-ϕ phase space but do not necessarily remain in close poximity with each other. Even for a perfectly isochronous machine, their energies diverge if their phases are different. For example if there are 100 turns to extraction, a particle 8° off crest takes an extra turn to reach the same energy (or radius). This mixes turns and reduces extraction efficiency for single turn extraction. A mitigation for maintaining phase acceptance is to "flat-top" the rf waveform by adding a third harmonic.

4.5.1 Stripping extraction machines

But for machines that extract by stripping, this is not an issue. These cyclotrons extract according to the particle's radius, not turn number, so it is immaterial whether one particle takes more turns than another.

TRIUMF example: A good but somewhat extreme example in this regard is the TRIUMF cyclotron. Its optimal particle needs roughly 1400 turns to reach 500 MeV, but the phase acceptance is as much as 60°, so the extreme phase takes 1600 turns (optimistically, on crest turns divided by 30° off-crest = $\cos 30°$). Thus extracted bunches typically have particles with a range of 1400 to 1600 turns. One of the consequences is that pulsing the beam at the ion source does not result in perfectly pulsed extracted beams: there are rise and fall times of 200 turns, or, at 4.6×10^6 turns per second, 43 μs.

Under the condition that particles are extracted when they reach a given energy, the integral in eqn. 4.8 is the same for all particles. We thus have that even for machines of poor isochronicity:

$$V_\mathrm{f} \sin \phi_\mathrm{f} - V_\mathrm{i} \sin \phi_\mathrm{i} = \text{constant} \tag{4.14}$$

[1] US patent number 8,207,656 B2

Exercise: It is typical for compact cyclotrons to inject 'off-crest'. This is because there is no vertical magnetic focusing at the centre of such machines; they rely upon electric focusing from the acceleration. But only particles injected when the energy gain is falling are vertically focused. There is then an isochronicity error (or 'field bump') that moves the centre of the bunch to be back on crest. For a case where particles are injected in a phase range from 0° to 60°, and for constant V, show that the final phase width shortens to 51°.

These machines have circulating particles occupying h (harmonic number) equidistant slots as if spokes of a wheel; each 'spoke' has an angular width roughly equal to the rf phase acceptance divided by the harmonic number h. If the turn betatron width, $\sqrt{\beta_x \varepsilon_x}$, is large compared with δR, the radius gain per turn (4.17), the radial turn density will be uniform. If not, individual turns will still be evident, but even in that case, if the extreme phase $\hat{\phi} > \sqrt{2/n}$ where n is turn number, then the extracted turns will be mixed.

Proof: To keep turns separate, need

$$nV \cos\hat{\phi} \approx nV(1 - \hat{\phi}^2/2) > (n-1)V, \text{ or, } 1/n > \hat{\phi}^2/2. \tag{4.15}$$

The extracted energy spread is very small and uncorrelated with particle phases. The energy spread arises from two sources: energy gain per turn and betatron amplitude. The energy gain per turn causes a particle just missing the foil to gain a full turn worth of energy before being extracted. This results in a dispersion correlation.[36] The dispersion D at the stripper foil is given directly by the need for orbit length to be proportional to particle speed $R \propto \beta$:

$$\frac{dR}{R} = \frac{1}{\gamma^2}\frac{dp}{p}, \text{ or, } D = \frac{R}{\gamma^2}. \tag{4.16}$$

From the stripper onward, the beamline can contain dipoles and be designed in such a way to compensate this dispersion. This has two advantages: it reduces beam size, and perhaps even more importantly, it makes the beam to first order insensitive to the stripper's radial position.[37] One often has a stripper that is only a few μm thick and no direct control over its radial position; it often warps or curls from use. So in such a case, the beamline does not need continuous retuning as the foil ages. Moreover, small energy changes can be made by moving the stripper radially, without retuning the beamline.

Since the stripper selects all particles at radius larger than the inner edge, the radial extent of the extracted beam is unrelated to the amplitude of radial betatron oscillation, and the extracted emittance can be smaller than the circulating emittance.

The phase space area is a parallelogram whose radial extent is the radius gain per turn,

$$\delta R = \frac{R}{\beta^2\gamma^2}\frac{\delta E}{E} = \frac{R_\infty}{\beta\gamma^3}\frac{\delta E}{mc^2}. \tag{4.17}$$

The divergence extent has two components that are uncorrelated: The divergence of the circulating beam, $x' = \sqrt{\varepsilon_x/\beta_x}$, and (refer to Fig. 4.2) the range of divergence resulting from the betatron motion of the accelerated equilibrium orbits of the range of particle phases: $x' = \delta R/\beta_x = \nu_x \delta R/R$. Usually, the former effect dominates. In that case we have that the extracted horizontal emittance ε_{ext} is smaller than the circulating emittance ε_x:

$$\varepsilon_{\text{ext}} = \delta R \sqrt{\varepsilon_x/\beta_x} \tag{4.18}$$

The vertical extracted emittance is the same as the circulating emittance. Here we have neglected the extra divergence that originates from scattering against the nuclei of the foil. The foil thickness can usually by chosen to be sufficiently small that this component is negligible. However, even though the contribution to the core emittance may be negligible, there may still be a sufficient number of large angle scatters to strike the beam pipe and cause activation unless collimated.

4.5.2 Single turn extraction machines

For the separated turn case, all particles remain in their turns with no mixing. It's clear from the foregoing that bunches extracted from a cyclotron can be customized by manipulating the functions $V(E)$ and $\omega(E)$: the phase width, the energy spread, and the phase-energy correlation follow from the Hamiltonian 4.8.

Let us first try the case of perfectly isochronous with constant V. Then

$$H(E, \phi; \theta) = \frac{qV}{2\pi} \sin\phi - \left(\frac{\omega_{\text{rf}}}{\omega_{\text{orbit}}} - h \right) (E - E_{\text{i}}) \tag{4.19}$$

and so $E' = (V/(2\pi)) \cos\phi$ and $\phi' = \omega_{\text{rf}}/\omega_{\text{orbit}} - h$. If ω_{rf} deviates from $h\omega_{\text{orbit}}$, the bunches' phase slips continuously and linearly with θ. Because of the nonlinearity of the rf waveform, the bunches in longitudinal phase space will be curved along ϕ if sufficiently long. The particles do not change phase relative to each other; they all slip by the same amount.

But isochronism is never perfect and besides, by means of correction coils, the function $\omega(E)$ can be tuned. In addition, the energy gain qV can be designed as a function of radius, a proxy for E. Knowing the functions $V(E)$ and $\omega(E)$, the equations of motion can be integrated for any particle. A useful technique is to apply conventional transfer matrix and 'Twiss' parameter formalism.

The full equations of motion are

$$\frac{d\phi}{d\theta} = -\frac{\partial H}{\partial E} = -q\frac{\sin\phi}{2\pi}\frac{dV}{dE} + \frac{\omega_{\rm rf}}{\omega(E)} - h \tag{4.20}$$

$$\frac{dE}{d\theta} = \frac{\partial H}{\partial \phi} = \frac{qV(E)}{2\pi}\cos\phi \tag{4.21}$$

Solving these once to find the reference particle coordinates functions $E_0(\theta)$ and $\phi_0(\theta)$, we then find motion relative to this reference, expanding H to second order in the differentials $\delta E = E - E_0(\theta)$, $\delta\phi = \phi - \phi_0(\theta)$. Making a canonical transformation to these differential coordinates involves simply expanding the Hamiltonian to second order and dropping first and lower order terms. We get:

$$H(\delta\phi, \delta E; \theta) = -\frac{qV}{2\pi}\sin\phi_0\,\frac{\delta\phi^2}{2} + \frac{qV'}{2\pi}\cos\phi_0\delta\phi\delta E + \left(\frac{qV''}{2\pi}\sin\phi_0 + 2\frac{\omega_{\rm rf}\omega'}{\omega^2}\right)\frac{\delta E^2}{2} \tag{4.22}$$

where all V, ω and their derivatives are evaluated at E_0. The equations of motion can be expressed in matrix form:

$$\frac{d}{d\theta}\begin{pmatrix}\delta\phi\\ \delta E\end{pmatrix} = \begin{pmatrix}\frac{-qV'}{2\pi}\cos\phi_0 & \frac{-qV''}{2\pi}\sin\phi_0 - \frac{2\omega_{\rm rf}\omega'}{\omega^2}\\ \frac{-qV}{2\pi}\sin\phi_0 & \frac{qV'}{2\pi}\cos\phi_0\end{pmatrix}\begin{pmatrix}\delta\phi\\ \delta E\end{pmatrix} \tag{4.23}$$

and integrated to find the transfer matrices and/or the Twiss β function as a function of turn number. This allows one to quickly find the longitudinal bunch envelope and energy width along the accelerating orbit as a function of the injected beam longitudinal sigma matrix or Twiss parameters.

For the perhaps more common case of no or negligible variation of V with E, we have more simply:

$$\frac{d}{d\theta}\begin{pmatrix}\delta\phi\\ \delta E\end{pmatrix} = \begin{pmatrix}0 & \frac{-2\omega_{\rm rf}\omega'}{\omega^2}\\ \frac{-qV}{2\pi}\sin\phi_0 & 0\end{pmatrix}\begin{pmatrix}\delta\phi\\ \delta E\end{pmatrix} \tag{4.24}$$

If perfectly isochronous, the 12 element also is zero, reflecting that an off-crest bunch gradually tilts. On crest ($\sin\phi_0 = 0$) with perfect isochronism and unchanging V, the whole matrix is zero and neither the phase width nor the energy width change. This is the usual (naïvely idealized) model of a cyclotron.

Gordon gives explicit formulas for the transfer matrix that apply under certain conditions.[33] Space charge cannot be included though, since it couples the longitudinal motion to the radial. This is dealt with in a separate chapter.

4.6 Higher order isochronism error

It has been known since early days that betatron motion affects a particle's phase. Intuitively, a trajectory that oscillates about a reference trajectory, as has more length than the reference trajectory. But it also follows in a simple way from the Hamiltonian dynamics. A good reference is the notes of Alex Chao[38]; in his words, *Chromaticities are therefore intimately related to the dynamics of the path length!*. This is because if transverse angle in action-angle coordinates depends upon energy through tune dependence, then through H, the 'action', being conjugate to angle, influences the time or rf phase as this phase is conjugate to energy. This seems to be rediscovered most often in analysis of isochronous or near-isochronous storage rings. An interesting case is the use of isochronism to obviate need for rf cavities in a storage ring[39]. More recently, Scott Berg has considered this for near-isochronous FFAs (such as EMMA), in particular because maintaining bunch integrity limits transverse acceptance.[40]

In our Hamiltonian, the lowest order transverse motion in action-angle coordinates ((J, ψ)as found in any textbook) and independent variable as distance along the orbit s is $J/\beta_T \approx J\nu/R$. There are terms for both x and y, ν is the tune, either x or y. To make independent variable the azimuth θ, it is to be multiplied by R: $H = J\nu$. This is an energy-time Hamiltonian, not energy phase; to make it so, it should be multiplied by $\omega_{\rm rf}$. We thus have the transverse H:

$$H_{\rm x,y}(J_x, \psi_x, J_y, \psi_y, \phi, E; \theta) = \omega_{\rm rf}(J_x\nu_x(E) + J_y\nu_y(E)). \tag{4.25}$$

The phase evolution due to this effect is

$$\frac{d\phi}{d\theta} = -\frac{\partial H}{\partial E} = -\omega_{\rm rf}\left(J_x\frac{d\nu_x}{dE} + J_y\frac{d\nu_y}{dE}\right) = -\frac{\pi}{\beta\lambda}(\varepsilon_x\xi_x + \varepsilon_y\xi_y), \tag{4.26}$$

where $\xi_{x,y}$ are the chromaticities defined in the usual way as $\frac{d\nu}{d(\Delta p/p)}$. The $\varepsilon_{x,y}$ are amplitudes written as usual x, x' emittances; they relate to the action as $\varepsilon_{x,y} = 2J_{x,y}/P_0$, where P_0 is the momentum $\beta E/c$. $\beta\lambda$ is the bucket separation; we thus find that bunches can smear into each other only after a number of turns of order of the ratio of bunch separation to emittance. This is a large number and no concern to cyclotrons where emittances are of order 10^{-6} m while $\beta\lambda \sim 1$ m. But in FFAs the harmonic number can be high and the transverse acceptance large. In scaling FFAs, the chromaticity is zero, so there is no issue with them.

Chapter 5

Space Charge

Space charge: At first, it was thought that the "pushed forward" particles at the head of a bunch would advance to higher radius and conversely the tail particles would go to smaller, thus tilting the bunches. This would have been easy to counteract: simply accelerate sufficiently off-crest that the tilt is compensated by the energy gain. What was not realized is that the same effect would cause particles at the low-radius side to advance in phase, and the high-radius particles would retard. The overall effect is to rotate the bunch in r, θ space. But remember that the bunches are already rotating, once per turn, about the cyclotron centre. We have been thinking in a rotating, noninertial reference frame. The space charge effect is to slow the intrinsic rotation frequency from once per turn to slightly less than 1. This shift when thought of in the radial direction is nothing other than the Laslett tune shift. The peculiarity of cyclotrons is that there is no longitudinal motion in this rotating frame. If the space charge force is linear, the bunches would simply rotate rigidly. But space charge is not linear except for very special and unrealistic bunch distributions; those with uniform density and hard edges. Instead, the density tends to be higher at the bunch centre tailing off into low density at the fringes. The bunch then will twist with the centre rotating faster than the fringes. This has much in common with tropical storms, typhoons or hurricanes: those also result from a central force acting in a rotating frame, the force is from a low pressure area, and the rotating frame is the earth. The result of this is that longish bunches will twirl like spaghetti around a fork, and if bunches are very long (roughly a factor of more than 3 times longer than their width), they can form two or more centres of rotation[41]. But if bunches are short and already circular in the (r, θ) plane, they will continue to be circular since it will not matter whether the outer particles in the bunch circulate more slowly than the inner ones. This effect, that there is a circular stationary distribution in cyclotrons, was discovered by ... and fully described by Wiel Kleeven[42].

Chapter 6

Resonances

As with other circular accelerators, cyclotrons' dynamics can be disrupted by orbit resonances. Ordinarily, regular periodic focusing, whether by regularly arranged separated quadrupoles, or by sector focusing, is a robust means to transport the particles through to higher energy. The linear fields result in harmonic motion. However, if the frequency of the motion matches the frequency of the focusing, resonance effects can occur. In this regard, cyclotrons are no different from synchrotrons. The theory developed especially by Guignard[43] is sufficiently general that it applies to cyclotrons as well. Lesser known but equally general, see Werner Joho's thesis (1970)[44]. The original theory, attributable to Poincaré but applied to accelerators by Moser[45], is given in Joho's thesis appendix, and the body of the thesis contains applications to the PSI 590 MeV ring cyclotron.

Compared with circular accelerators in general, cyclotrons are a niche application because of the following characteristics.

- The horizontal tune is forced to ramp through resonances, since the requirement for isochronism results in a tune increasing monotonically with energy, and in fact roughly is close to γ. (But see Planche (2019)[46] for unusual designs where this rule is broken.)
- As average magnetic field on a given orbit is proportional to γ, average second and higher field derivatives are necessarily non-zero.
- Small cyclotrons, injected at $\gamma = 1$ are effectively already on the $\nu_x = 1$ integer resonance, and the 2/2 half-integer resonance.
- As well small cyclotrons have very little vertical focusing at injection since the sector focusing cannot exist at zero radius. This means in effect that injection at low energy is always at near $\nu_z = 0$. The space charge limit depends upon mitigating

this "resonance".

- Accelerating gaps, also being periodic, can drive resonances in a similar way to synchrobetatron resonances in synchrotrons. But the gaps are often not in magnetic field-free regions and not oriented along the reference orbit, resulting in transverse kicks. These can drive resonances.

6.1 Fast passage theory

It is not difficult to "back out" the Hamiltonian of linear motion about the equilibrium orbit from the equations 3.46, 3.47, once the equilibrium orbit has been found:

$$\mathcal{H}(x, p_x; \theta) = \frac{rp^2}{p_\theta^3} \frac{p_x^2}{2} + \frac{p_r}{p_\theta} x p_x + q \frac{\partial}{\partial r}(rB) \frac{x^2}{2}. \tag{6.1}$$

No zero order motion terms linear in (x, p_x) appear, since we know that $(x, p_x) = (0, 0)$ has to be a solution.

Exercise: Perform the canonical transformation from (r, p_r) to (x, p_x) where $r = r_{\rm EO} + x$, $p_r = p_{r\rm EO} + p_x$ to get the new Hamiltonian in this way. Hint: the generating function is

$$F(r, p_x; \theta) = [r - r_{\rm EO}(\theta)] \; p_x + r \; p_{r\rm EO}(\theta). \tag{6.2}$$

6.1.1 Back to the Frenet-Serret coordinate system

Remember that (x, p_x) are **radial** coordinates not Frenet-Serret coordinates as they would be for a synchrotron. We could transform to the Frenet-Serret coordinate $x_{\rm FS}$ knowing

$$\frac{x_{\rm FS}}{x} = \frac{p_\theta}{p} \tag{6.3}$$

or even more directly by going back to the basic Hamiltonian 3.7 and linearizing. But that has already been done for us; it is the analysis long known since Courant and Snyder [17], and we can capitalize on it now that we know the equilibrium orbit. The linearized equations of motion are both of the Mathieu-Hill type[47]:

$$y'' + K(s)y = 0. \tag{6.4}$$

As in the FS coordinate system, the path length along the reference trajectory, s, is the independent variable, the **primes now denote derivatives with respect to** s. The

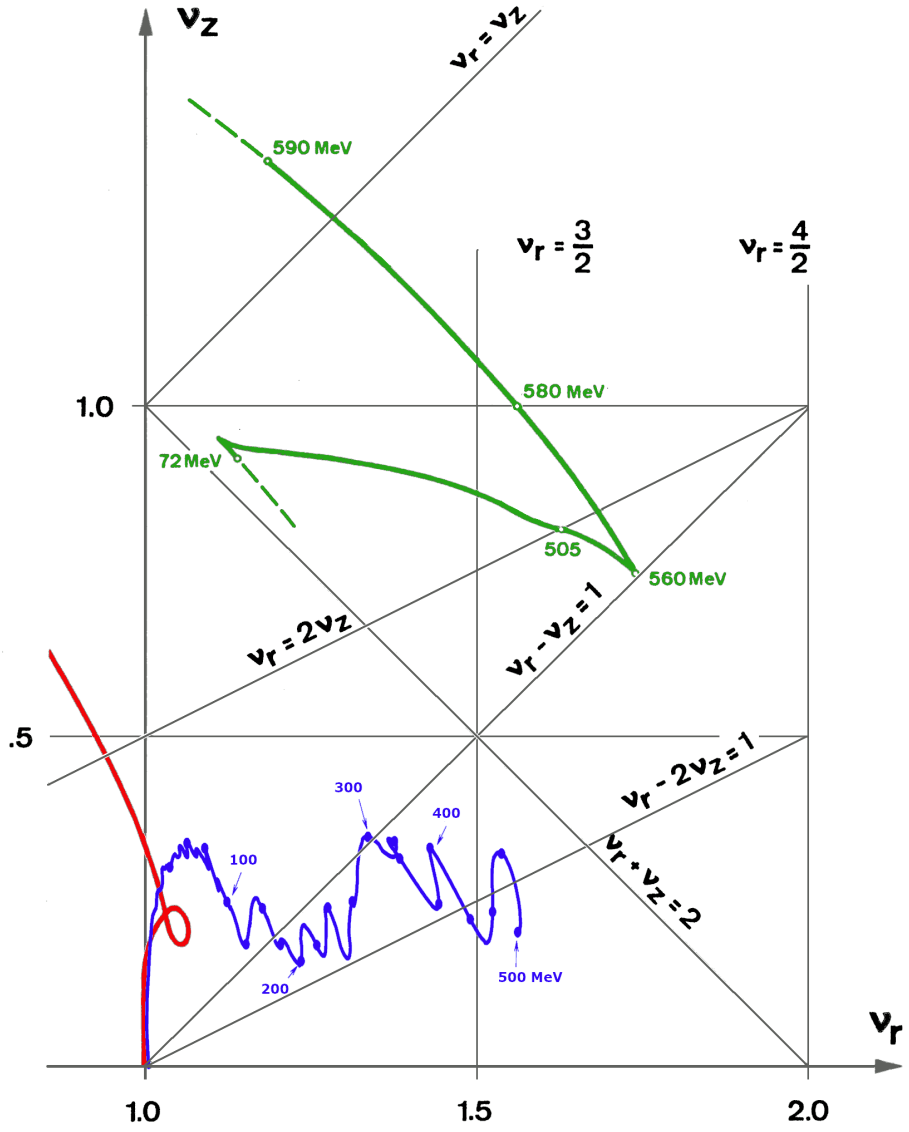

Figure 6.1: A sampling of three machines' tunes displayed on a tune diagram. Green: PSI 590 MeV ring cyclotron. Blue: the TRIUMF 500 MeV cyclotron. Red: MSU's 50 MeV proton cyclotron. Notice the ring cyclotron has a relatively far larger vertical tune, while others start with vertical tune near zero at injection. Both high energy machines traverse the $\nu_x = 3/2$ resonance. The MSU and PSI machines traverse the Walkinshaw resonance $\nu_x = 2\nu_z$.

x coordinate is no longer radial, but now orthogonal to the reference path. The vertical coordinate z is unchanged.

For radial motion, $K(s) = k_x(s) = \frac{1+k}{\rho^2}$, and for vertical, $K(s) = k_z(s) = \frac{-k}{\rho^2}$. Both parameters k and $\rho = p/(qB(s))$ are functions of s; k is the **local** field index introduced in a previous section:

$$k = \frac{\rho}{B}\frac{\partial B}{\partial x} \tag{6.5}$$

evaluated at the equilibrium orbit $x = 0$.

The Hamiltonian for x is simply

$$\mathcal{H}(x, p_x; s) = \frac{p_x^2}{2} + \frac{k_x x^2}{2}. \tag{6.6}$$

Here, p_x is in units of the reference momentum $p = qB\rho$. This results in an equation of motion

$$x'' + k_x x = 0. \tag{6.7}$$

To the regular radial motion we add a term arising from field error δB. This contributes δp_x,

$$\frac{d(\delta p_x)}{dt} = \frac{qv\delta B}{p}, \ \frac{d(\delta p_x)}{ds} = \frac{q\delta B}{p} = \frac{\delta B}{B\rho}. \tag{6.8}$$

The equation of motion becomes

$$x'' + k_x x = \frac{\delta B}{B\rho}. \tag{6.9}$$

As is well-known (and again, first derived by Courant and Snyder[17], the homogeneous solution can be written

$$x = \sqrt{\beta}\cos(\nu\theta + \psi), \text{ where } \theta := \int \frac{ds}{\nu\beta}, \tag{6.10}$$

β being of course the well-known "Courant-Snyder" (or "Twiss") parameter and ν the tune. And we can re-write the equation of motion as one of a driven simple harmonic oscillator with normalized coordinate $\eta = \beta^{-1/2}x$:

$$\frac{d^2\eta}{d\theta^2} + \nu^2\eta = \nu^2\beta^{3/2}\frac{\delta B}{B\rho} \tag{6.11}$$

6.1.2 Smooth-focus approximation

For simplicity and more clarity at the expense of a little accuracy, we will use a smooth-focusing, constant $\beta = \frac{\mathcal{R}}{\nu}$ version of this equation,

$$\frac{d^2x}{d\theta^2} + \nu^2 x = \mathcal{R}^2 \frac{\delta B}{B\rho}, \tag{6.12}$$

but keeping in mind that the more accurate version has this $\beta^{3/2}$ weighting of the error field. Note that we introduced a "radius" of the orbit, which is in fact the orbit length L divided by 2π. Further, this θ is not (quite) the same as the old one, namely the cylindircal coordinate azimuth. Instead it is $\theta = s/\mathcal{R} = 2\pi s/L$. The Hamiltonian is

$$\mathcal{H}(x, \tilde{p}; \theta) = \frac{\tilde{p}^2}{2} + \nu^2 \frac{x^2}{2} + \frac{\mathcal{R}^2}{B\rho} \int \delta B dx \tag{6.13}$$

To keep it uncluttered, we simply redefine a momentum: $\tilde{p} := \mathcal{R}\frac{p_x}{p}$.

In anticipation of the resonant behaviour, we write δB as a Taylor expansion in x and a Fourier expansion in θ.

$$\delta B(x, \theta) = \sum_{m=1}^{\infty} \sum_{n=0}^{\infty} \frac{1}{n!} \frac{\partial^n B_m}{\partial x^n} x^n \cos(m\theta + \theta_m), \tag{6.14}$$

where B_m is the m^{th} Fourier component.

As will become clear, only one of the terms in the expansion is resonant at one time, so we write the Hamiltonian as

$$H = \frac{\tilde{p}^2}{2} + \frac{\nu^2 x^2}{2} + m\frac{b_{mn} x^n}{n} \cos(m\theta + \theta_m) \tag{6.15}$$

where

$$m b_{m,n+1} := \frac{\mathcal{R}^2}{B\rho} \frac{1}{n!} \frac{\partial^n B_m}{\partial x^n} \tag{6.16}$$

This is a driven simple harmonic oscillator, which will have resonances depending upon a relation between ν, m, and n. As the beam accelerates, the tune ν changes, to first order as $\nu(\theta) = \nu_0 + \nu'\theta$, passing through resonances.

The usual approach is to transform to action-angle coordinates (J, ψ):

$$x = \sqrt{2J/\nu} \cos\psi, \ \tilde{p} = \sqrt{2J\nu} \sin\psi \tag{6.17}$$

The transformed Hamiltonian:

$$H = \nu J + \frac{m b_{mn}}{n} \left(\frac{2J}{\nu}\right)^{n/2} \cos^n\psi \cos(m\theta + \theta_m) \tag{6.18}$$

6.1.3 Solution

$$J' = mb_{mn}\left(\frac{2J}{\nu_0}\right)^{n/2}\cos^{n-1}\psi\sin\psi\cos(m\theta+\theta_m), \tag{6.19}$$

or, expanding the trig powers,

$$J' = mb_{mn}\left(\frac{J}{2\nu_0}\right)^{n/2}[\sin(n\psi - m\theta - \theta_m) + \text{ other terms}] \tag{6.20}$$

We retain the designated term because it is the only one with slow variation with θ, and does so when the resonance condition

$$n\nu_0 = m \tag{6.21}$$

is met; the other terms will vary too rapidly to make a net contribution.

The naïve approach would be to assume there are some particles at the worst phase and set the sine to 1 and integrate J to find the growth over a finite time, for instance over the time it takes to pass through the stopband. Or half that time since the growth rate varies between zero and maximum through the stopband. This would be correct for fixed tune or for rate of change of tune to be very small compared with the amplitude growth rate. It is not true in general. Instead of fixed ψ, we have a quadratic function of θ:

$$\psi' = \frac{\partial H}{\partial J} = \nu + \text{ oscillatory term} \tag{6.22}$$

$$\psi \approx \int \nu d\theta = \nu_0\theta + \nu'\theta^2/2. \tag{6.23}$$

$$n\psi - m\theta = n[\nu_0\theta + \nu'\theta^2/2] - m\theta = n\nu'\theta^2/2. \tag{6.24}$$

The action equation is a little simpler if we revert to $A = \sqrt{2J/\nu_0}$, the betatron amplitude:

$$\frac{A'}{A^{n-1}} = \frac{mb_{mn}}{2^n\nu_0}\sin(n\nu'\theta^2/2 - \theta_m) \tag{6.25}$$

We see that we get a Fresnel integral. The largest amplitude gain occurs for phase $\theta_m = \pi/4$:

$$\frac{\Delta(A^{2-n})}{2-n} = \frac{mb_{mn}}{2^n\nu_0}\sqrt{\frac{2\pi}{n\nu'}} \tag{6.26}$$

Note $\nu_0 = m/n$. Also, we prefer the tune change per turn, $\nu_\tau \equiv 2\pi\nu'$,

$$\frac{\Delta(A^{2-n})}{2-n} = \frac{\pi}{2^{n-1}}b_{mn}\sqrt{\frac{n}{\nu_\tau}} \tag{6.27}$$

Of course this does not hold for $n = 2$; in that case, the LHS is $\Delta(\log A)$.

It is interesting to compare this with the slow passage version where we set the sine in eq. 6.25 to 1/2. Then we find

$$\frac{\Delta(A^{2-n})}{2-n} = \frac{mb_{mn}}{2^n\nu_0}\frac{\Delta\theta}{2} = \frac{nb_{mn}}{2^n\nu_0}\frac{\pi\Delta\nu}{\nu_\tau}. \tag{6.28}$$

Another way to view this result is that the resonance width $\Delta\nu$ is replaced by an effective width

$$\text{“}\Delta\nu\text{”} = 2\sqrt{\frac{\nu_\tau}{n}}, \tag{6.29}$$

and the actual stopband width becomes irrelevant.

6.1.4 Guignard's (exact) formula

Guignard[43] uses the full equation 6.11 and so is more precise. Our formula agrees with his for the constant Twiss β case except that he would have $\pi^{n/2}$ in place of our π (note that Guignard's E is actually $\pi\epsilon$). From this we can generalize the definition of b_{mn} to non-smooth focusing. Since in the non-smooth case, A is ambiguous, we revert to expression in terms of the particle's emittance ϵ.

$$\left|\frac{\Delta(\epsilon^{1-n/2})}{n-2}\right| = \frac{\pi}{\sqrt{n\nu_\tau}}\frac{\mathcal{R}}{2^{n-2}\,B\rho}\left|\frac{1}{2\pi}\int_0^{2\pi}\frac{\beta_x^{n/2}}{(n-1)!}\frac{\partial^{n-1}\delta B}{\partial x^{n-1}}\,e^{im\theta}\,d\theta\right| \tag{6.30}$$

The important difference from the smooth case is that the Fourier component of δB is weighted by the β-function to the power $n/2$. Field errors are magnified where betatron amplitude is larger, and this dependence increases for increasing resonance order.

6.2 Integer resonance

6.2.1 Radial

If a small first harmonic is added to a completely flat field, orbiting particles will drift perpendicular to the field gradient, because where the field is too high, they will curve too much and where low, too little. There is no stability. This is the case for the first few turns in a small cyclotron where $\nu_x = 1$. If the field rises according to $B \propto \gamma \approx 1 + \beta^2/2$, it is parabolic in R and a first harmonic simply shifts the minimum of the parabola.

More generally, for any harmonic m, $\nu_x = m$ causes a coherent oscillation. Passing quickly through the resonance, we can apply the above formula:

$$\Delta A = \pi \frac{b_{m,1}}{\sqrt{\nu_\tau}} = \frac{\pi}{\sqrt{\nu_\tau}} \frac{\mathcal{R}^2}{B\rho} \frac{B_m}{\nu} \tag{6.31}$$

The effect is to cause an m-fold sinusoidal orbit displacement or distortion. At injection in a small cyclotron, $\nu_x \approx 1$ and the "closed orbit distortion" is to simply off-centre the circular orbit. It was also often used to create a coherent oscillation to help extract the beam. See for example Garren et al.[48].

Exercise: Take a simple case where beam is injected into a compact proton cyclotron. Find the static orbit shift assuming an isochronous field. Now also find the fast passage shift given by the above formula, assuming energy gain per turn is 100 keV.

6.2.2 Vertical

A ring cyclotron such as the PSI 590 MeV machine has enough vertical focusing that it passes through the $\nu_z = 1$ integer tune. This is driven by the first harmonic of radial error field on the median plane, effectively tilting it. The formula is exactly the same as eqn. 6.31, with $b_{m,1}$ being the radial first harmonic.

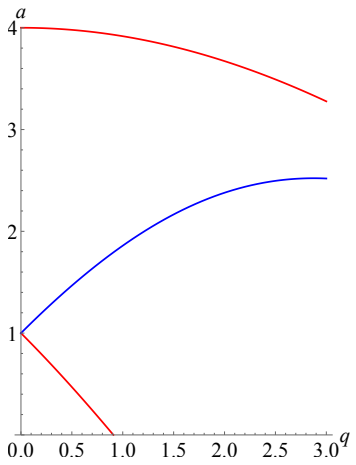

Figure 6.2: Mathieu equation stability region near $a = 1$. The region between the red and the blue curves is unstable and at any given q, the distance between them is the stopband width.

6.3 Half-integer

The formula

$$\log \frac{A_\mathrm{f}}{A_\mathrm{i}} = \frac{\pi}{\sqrt{2}} \frac{b_{m,2}}{\sqrt{\nu_\tau}} \tag{6.32}$$

was verified experimentally in the TRIUMF cyclotron[49]. $b_{m,2} = \frac{\overline{\mathcal{R}}}{m\overline{B}} \frac{\partial B_m}{\partial x}$, where $m = 2\nu$. Small cyclotrons are susceptible at injection where $\nu_x = 1 = 2/2$: the driving force is from the second harmonic of the gradient of the magnetic field. The largest cyclotrons, PSI and TRIUMF, surpass $\gamma = 1.5$ and therefore cross the 3/2 resonance. The effect is to cause a mismatch, stretching the beam ellipse.

Exercise: Repeat the exercise above, but for the 2/2 resonance. Assume the second harmonic of the magnetic field scales with the zeroth harmonic, which necessarily is proportional to γ.

6.3.1 Stopbands

The concept of stopband can be applied to any order n resonance: it is the range of tunes for which the motion is unstable. However, it has a "clean" definition only in the case of $n = 2$. In the other cases, the stopband depends on the particles' amplitude of oscillation. In the half-integer case, the stopband is independent of particle motion, and the tune has an imaginary part inside it. Thus, one can find a rate of growth of mismatch inside the stopband, multiply by the time taken to cross through it, to get the total growth. This would be called a "static" rather than a fast-passage approach, and it is incorrect for most cases of interest. Let us look again at the bare equation of motion:

$$\frac{d^2x}{d\theta^2} + (\nu^2 - mb_{m,2}\cos m\theta)x = 0, \tag{6.33}$$

or, in Frenet-Serret form:

$$x'' + \left[\left(\frac{\nu}{\mathcal{R}}\right)^2 - \frac{mb_{m,2}}{\mathcal{R}^2}\cos\left(\frac{ms}{\mathcal{R}}\right)\right]x = 0 \tag{6.34}$$

This is the classic Mathieu equation; there is an unstable region within a band around $\nu = m/2$. To make the identification with the standard form $\frac{d^2x}{dv^2} + (a - 2q\cos 2v)x = 0$ we note that $a = \left(\frac{\nu}{m/2}\right)^2$ and $q = \frac{2b_{m,2}}{m}$, $2v = \frac{ms}{\mathcal{R}} = m\theta$.

See Fig. 6.2. To a good approximation for small q, the stopband is $1 - q < a < 1 + q$, meaning

$$\nu^2 = \left(\frac{m}{2}\right)^2 \pm \frac{m}{2}b_{m,2} \tag{6.35}$$

are the stopband edges.

But there's a better and easier way to solve equation 6.33. It is not important that the perturbation be exactly sinusoidal, if the perturbation is small enough that the tune changes by an increment much smaller than 1. We can replace it by two Dirac δ-functions half a period apart, each being a thin lens of focal length f. Then we can analyze using standard matrix optics. The sequence is

$$\begin{pmatrix} \cos\mu^\star & \beta_x^\star \sin\mu^\star \\ \frac{\sin\mu^\star}{-\beta_x^\star} & \cos\mu^\star \end{pmatrix} = \begin{pmatrix} \cos\mu/2 & \beta_x\sin\mu/2 \\ \frac{\sin\mu/2}{-\beta_x} & \cos\mu/2 \end{pmatrix} \begin{pmatrix} 1 & 0 \\ \frac{1}{f} & 1 \end{pmatrix} \begin{pmatrix} \cos\mu/2 & \beta_x\sin\mu/2 \\ \frac{\sin\mu/2}{-\beta_x} & \cos\mu/2 \end{pmatrix} \begin{pmatrix} 1 & 0 \\ \frac{1}{-f} & 1 \end{pmatrix} \tag{6.36}$$

Here, β_x is the Courant-Snyder β-function, equal to $\mathcal{R}/\nu$ in this smooth approximation, $\mu = \nu\theta = 2\pi\nu/m$, the betatron phase advance for one period of the perturbation. The starred parameters are the perturbed ones. Plotted using Mathematica, the result is displayed in Fig. 6.3.

The tune being near $m/2$, μ is near π so we can expand the trig functions. To a good approximation, the result is

$$\left(\nu^\star - \frac{m}{2}\right)^2 = \left(\nu - \frac{m}{2}\right)^2 - \left(\frac{m\beta_x}{2\pi f}\right)^2 \tag{6.37}$$

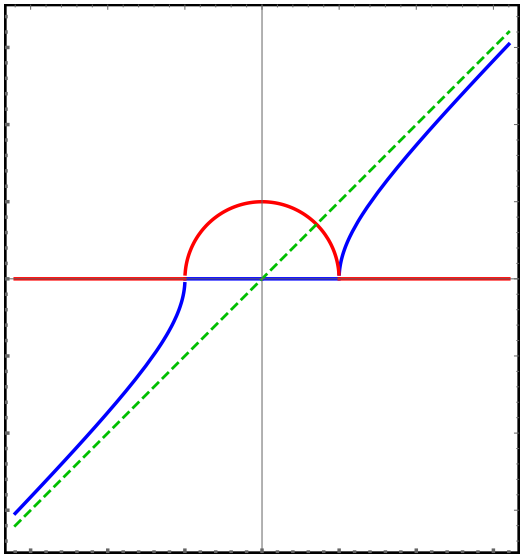

Figure 6.3: Tune $\nu^\star$ plotted against unperturbed tune ν near a half-integer resonance. The real part is Blue, the imaginary part is Red. The unperturbed tune, where the n-harmonic of the gradient field is zero, is in Green. Notice that the stopband half width is equal to the imaginary part maximum, resulting in the imaginary part being a near exact circle.

It remains to find the Fourier component of the field gradient for the lenses of focal length f. The field gradient from a single thin quadrupole of focal length f at path location $s = s_i$ is $\frac{dB}{dx} = \pm\frac{B\rho}{f}\delta(s - s_i)$. Around the orbit, we have such quadrupoles alternating in sign, equally spaced apart by $\frac{\pi\mathcal{R}}{m}$. We thus have

$$\frac{dB_m}{dx} = \frac{1}{\pi}\int_{-\pi}^{\pi}\frac{dB}{dx}\sin(m\theta + \theta_m)d\theta = \frac{1}{\pi\mathcal{R}}\int_{-\pi\mathcal{R}}^{\pi\mathcal{R}}\frac{dB}{dx}\sin\left(\frac{ms}{\mathcal{R}} + \theta_m\right)ds \tag{6.38}$$

The δ-functions are placed with respect to θ_m to maximize this integral, and we find finally (refer to definition 6.16):

$$b_{m,2} = \frac{2\mathcal{R}}{\pi f} \tag{6.39}$$

Using this and $2\nu \approx m$, the tune equation 6.37 is

$$\left(\nu^\star - \frac{m}{2}\right)^2 = \left(\nu - \frac{m}{2}\right)^2 - \left(\frac{b_{m,2}}{2}\right)^2 \tag{6.40}$$

Within the approximation, this is consistent with 6.35, and moreover gives the imaginary part of the tune: exactly on resonance, it is $b_{m,2}/2$, dropping to zero at the stopband edges. The stopband extends from $\nu = m/2 - b_{m,2}/2$ to $\nu = m/2 + b_{m,2}/2$; width is $b_{m,2}$. The imaginary part of the tune $\nu^\star$, plotted as a function the unperturbed tune ν is a circle of radius $b_{m,2}/2$ centred on $n/2$.

As an imaginary part of the tune results in exponentially growing betatron amplitude, we can use it to calculate the total growth on slow or adiabatic passage. The result is

$$\log \frac{A_\mathrm{f}}{A_\mathrm{i}} = \left(\frac{\pi}{2}\right)^2 \frac{b_{m,2}^2}{\nu_\tau} \tag{6.41}$$

This is, with a factor of 2, the **square** of the fast passage result 6.32. Upon fast passage, the dominant effect is the mismatch that results from the matched β-function changing non-adiabatically. See Baartman et al.[49] for more details and experimental verification.

Exercise: Show by extending the above matrix treatment, that the Courant-Snyder β-function diverges at the edges of the stopband.

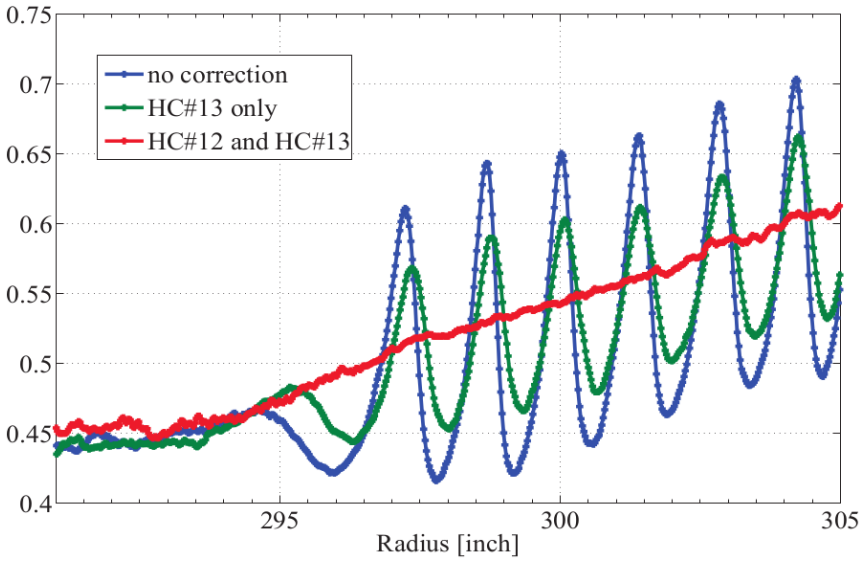

Figure 6.4: Radial current density modulation in the TRIUMF cyclotron, on passage through the 3/2 resonance. For the green curve, only one harmonic coil set (HC) is used and its phase is fixed and not appropriate for correction. But because the neighbouring coils 12 and 13 are azimuthally displaced, a combination of their currents could be found whose vector sum achieved correction (red curve, from [50]).

The TRIUMF 520 MeV cyclotron traverses the 3/2 resonance at 428 MeV. The third harmonic of the magnetic field is small but not negligible. It was known through simulations[51]

that a third harmonic field gradient of 8 G/m would more than double the circulating emittance. Shimming reduced it to approximately this level and it was sufficient for most purposes. However, later operation of simultaneous beams extracted from the cyclotron at energies beyond the resonance required to reduce it further. The effect of the resonance is to cause a modulation radially of the beam density, making the fraction split between the two beamlines sensitive to very small fluctuations in acceleration voltage. The needed reduction was achieved by re-wiring the correction coils, which had been wired to provide only a first harmonic, to provide also a third harmonic of appropriate phase.[52, 50]

6.3.2 Intrinsics

An intrinsic half-integer resonance at $\nu = m/2$ occurs when the harmonic m is a multiple of the cyclotron periodicity; its number of sectors N. This is generally impassable. The resonance 2/2 is an intrinsic resonance and prohibits any cyclotron of just two sectors. The next possibility is 3/2 for a 3-sectored cyclotron.

For separate sectors, the dominant component is as large as the average magnetic field. So $B_3 \sim \overline{B}$. But the gradient must be enough to satisfy isochronism and this means $\overline{B} \propto \gamma$, $\mathcal{R} \propto \beta$. Applying to 6.16, we get $b_{3,2} = (\gamma^2 - 1)/3$. The edge of the stopband is at $\nu = \gamma = 3/2 - b_{3,2}$ giving a quadratic equation for largest possible γ. This turns out to be $\sqrt{19} - 3 = 1.35$ for a proton energy of 335 MeV. In fact a detailed calculation finds the effect of the resonance to be much worse because, as noted above, the β-function diverges at the stopband edge. Kleeven has found an upper limit of only 185 MeV for 3-sectored proton cyclotrons[53].

The TRIUMF cyclotron has 6 sectors so the 6/4 resonance is intrinsic and simultaneous with the 3/2. The effect is to cause four unstable fixed points to appear and these travel through the stable fixed point during resonance crossing, sufficiently quickly at 0.4 MeV energy gain per turn, that the effect is negligible (see Fig. 6.5).

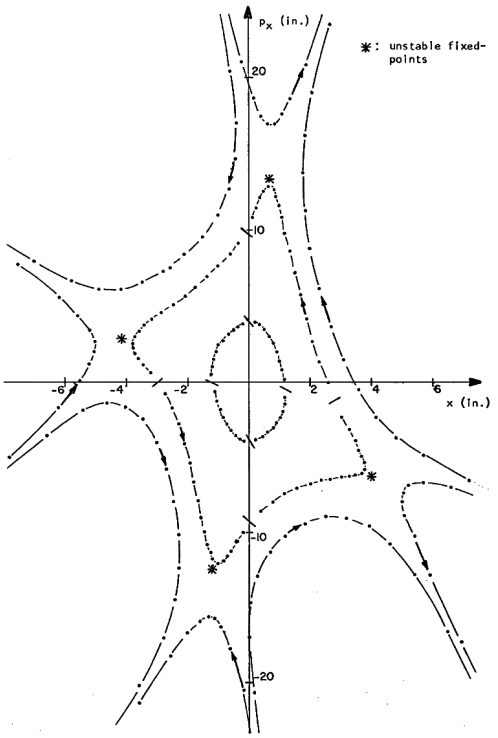

Figure 6.5: Phase space trajectories near the TRIUMF intrinsic 6/4 resonance (from [51]).

6.3.3 Vertical half-integer

Again, the vertical case is the same as the radial. Even the field expressions are the same since by $\nabla \times \vec{B} = 0$, we have $\frac{\partial B_z}{\partial x} = \frac{\partial B_x}{\partial z}$.

6.4 1/3-integer

$$\Delta\left(\frac{1}{A}\right) = \frac{\sqrt{3}\,\pi}{4}\,\frac{b_{m,3}}{\sqrt{\nu_\tau}} \tag{6.42}$$

or, more precisely,

$$\Delta\,\epsilon^{-1/2} = \frac{\pi}{4\sqrt{3}}\,\frac{1}{\sqrt{\nu_\tau}}\,\frac{\mathcal{R}}{B\rho}\left|\beta_x^{3/2}\,\frac{\partial^2 \delta B}{\partial x^2}\right|_{m=3\nu} \tag{6.43}$$

The trend for resonances is that they are less dangerous the higher the order, so one would expect the imperfection third order resonances to be easily crossed. However, most proposed muon FFAGs traverse a cell tune of 1/3. This is the **intrinsic** resonance $3\nu = N_{\text{cells}}$. Even a slight systematic sextupole component will result in very large $b_{m,3}$ when $m = N_{\text{cells}}$.

Exercise: For a 9 GeV proton cyclotron with 30 sectors, 25 MeV energy gain per turn, $\mathcal{R} = 20\,\text{m}$, use method above for the intrinsic half-integer resonance to estimate emittance growth through $\nu = 10 = 30/3$ resonance. Compare with simulation presented in the 1983 paper [54].

Resonances of order higher than 3 are generally not dangerous, even if intrinsic. The TRIUMF cyclotron safely and easily crosses the intrinsic 6/4 resonance, though it is simultaneous with the 3/2 resonance[51].

6.5 Coupling Resonances

6.5.1 Historical note

One can find a first full treatment of coupling resonances in CERN report by Hagedorn and Schoch[55, 56, 57], though these owed much to simultaneous work at MURA. Both owe much to even earlier work, predating the application to accelerators. Coupled harmonic oscillators were treated already around 1900, by for example Korteweg[58], Beth[59, 60]. Birkhoff (1927) developed a general approach that was adapted by Moser (1955) to circular accelerator applications, with contributions from the MURA physicists especially Keith Symon and Jackson Laslett. Between CERN and MURA, along with other cyclotron labs

such as Harwell, there was a flurry of activity all in the mid 50s; see especially the conference of High Energy Accelerators of 1959 where Meier and Symon report[61]. In the mid-70s, Guignard summarized the known theory to make it more accessible to accelerator designers who were not necessarily specialists in orbit theory[62, 43].

6.5.2 General theory

The most important coupling resonances for cyclotrons are the linear coupling $\nu_x - \nu_z = 1$, and the "Walkinshaw" resonance $\nu_x - 2\nu_z = 0$. See Fig. 6.1. The former is driven by error fields that are radial and break the median plane symmetry, while the latter, though third order, is dangerous because it is intrinsic for any number of sectors, as it is driven by the average field or zeroth harmonic.

The theory above can be generalized to coupling resonances. We define positive integers n_x, n_z, m as referring to the resonance

$$n_x\nu_x \pm n_z\nu_z = m. \tag{6.44}$$

The "order" of the resonance is $n_x + n_z$. The driving fields are derivatives of the magnetic field of periodicity m. There are two action-angle pairs involved: (ψ_x, J_x), (ψ_z, J_z). The Hamiltonian is a sum of the harmonic oscillator terms, both x and z, and a perturbed part $\mathcal{H}_1$:

$$\mathcal{H} = \frac{p_x^2}{2} + \nu_x^2\frac{x^2}{2} + \frac{p_z^2}{2} + \nu_z^2\frac{z^2}{2} + \mathcal{H}_1 \tag{6.45}$$

The perturbation is written as a 2D Taylor series in powers of x and z whose coefficients are the field derivatives evaluated at the equilibrium orbit. Unperturbed, the x and z motions are simple harmonic ($x = \sqrt{\frac{2J_x}{\nu_x}}\cos(\psi_x - \nu_x\theta)$, $p_x = \sqrt{2J_x\nu_x}\sin(\psi_x - \nu_x\theta)$, etc.) and so result in powers of cosines and sines. The field derivatives in turn are expanded as a Fourier series. Of this triple sum, we retain only the one term that has a nearly constant oscillatory part resulting from the tunes satisfying the resonance condition eqn. 6.44. The result is:

$$\mathcal{H}_1 = a_m \left(\frac{J_x}{2\nu_x}\right)^{n_x/2} \left(\frac{J_z}{2\nu_z}\right)^{n_z/2} \cos(n_x\psi_x \pm n_z\psi_z - m\theta_0), \tag{6.46}$$

where:

$$a_m = a_m(n_x, n_z) = \frac{2}{n_x!n_z!}\,\frac{1}{2\pi}\frac{\mathcal{R}^2}{B\rho}\int_0^{2\pi} \frac{\partial^{n_x+n_z-1}B_{(x|z)}}{\partial x^{n_x+n_z-1}} \exp[im\theta]d\theta. \tag{6.47}$$

The notation $B_{(x|z)}$ means we take the radial or x-component of $\vec{B}$ if n_z is odd, and the vertical or z-component if it is even. This can be recognized as respectively the "skew" and "normal" multipole components of the magnetic field. The interested reader can find more details of the derivation and a more precise final result that does not make use of the

smooth approximation and integrates instead over the varying Courant-Snyder parameters, in the CERN yellow report[43, section 8.1].

As shown by many authors, the resultant motion has a new invariant $n_x J_z \mp n_z J_x$. We prefer to write this as

$$\frac{J_x}{n_x} \mp \frac{J_z}{n_z} = J_0, \tag{6.48}$$

where J_0 is a constant. Actions are positive definite and so can grow without limit for sum resonances since only their difference is a constant. Actions on difference resonances are bounded, but can nevertheless be inconvenient. For example in the TRIUMF cyclotron, losses and activation are caused by difference coupling resonances, in the following way. It is not possible to trim the radial circulating emittance in a cyclotron, so large amplitude particles are carried to high energy. But it is a simple matter to dump large vertical betatron amplitude particles at a low, harmless energy. However, passages through coupling resonances ($\nu_x - \nu_z = 1$ and perhaps $\nu_x - 2\nu_z = 1$, see Fig. 6.1) cause vertical halo to reappear.

Joho[44] derives the following parameter that he calls the "critical frequency" κ.

$$\kappa = |a_m| \left(\frac{n_x}{2\nu_x}\right)^{n_x/2} \left(\frac{n_z}{2\nu_z}\right)^{n_z/2} |J_0|^{\frac{n_x+n_z}{2}-1} \tag{6.49}$$

Notice that for order $n_x + n_z = 2$, or linear resonances, the dependence upon action disappears. This can be related to the stopband width, see Guignard[43], but for the reason given below, the stopband is not usually the main concern.

The motions of the two degrees of freedom will couple if the distance from the resonance, $\Delta\nu := |n_x\nu_x \pm n_z\nu_z| - m$ is less than κ. A clever technique to solve the 4-dimensional coupled phase space problem is to use the new invariant eqn. 6.44 to make a canonical transformation to two dimensions. Normalizing the action as

$$\rho_x := \frac{J_x}{n_x|J_0|} \text{ and } \rho_z := \frac{J_z}{n_z|J_0|} \text{ with } |\rho_x \mp \rho_z| = 1, \tag{6.50}$$

and angle as

$$\Phi := n_x\psi_x \pm n_z\psi_z - m\theta_0, \tag{6.51}$$

the Hamiltonian will have the canonical pair (Φ, ρ_x):

$$\mathcal{H}(\rho_x, \Phi; \theta) = -\Delta\nu\rho_x - \kappa\rho_x^{n_x/2}(1 \pm \rho_x)^{n_z/2} \cos\Phi \tag{6.52}$$

(Note well that $\rho_z' = \pm\rho_x'$ so we only need to solve for one of them: ρ_x. We could just as well interchange x and z and solve for ρ_z.)

The upper sign is for sum resonances, and the lower is for difference. Trajectories are easily found by numerical integration for any particular resonance, plotted below for a particular case, but a few more general remarks can be made for weak resonances.

In a cyclotron, it is often undesirable to have any mixing of the radial motion into the vertical, because the magnet gap is more restrictive than the radial acceptance. Or vice versa, for machines that extract using a radial betatron excitation, it may be undesirable to have the vertical emittance "leak into" and increase the radial emittance. Starting a particle with pure z motion, $\rho_z = 1$, $\rho_x \ll 1$, we initially have maximum growth

$$\rho_x' = \kappa \rho_x^{n_x/2} (1 \pm \rho_x)^{n_z/2} \sin\Phi \sim \kappa \rho_x^{n_x/2} \tag{6.53}$$

Similarly, if a particle has near pure radial motion,

$$\rho_z' = \kappa \rho_z^{n_z/2} (1 \pm \rho_z)^{n_x/2} \sin\Phi \sim \kappa \rho_z^{n_z/2} \tag{6.54}$$

It is tempting to integrate these as $\frac{\Delta\rho^{1-n/2}}{1-n/2} = \kappa\Delta\theta$ for some stopband width that requires $\frac{\Delta\theta}{2\pi}$ turns to traverse, and take this is the maximum total growth. But as with the one-dimensional case, this would be incorrect. The phase Φ is varying as the resonance is traversed, according to $\Phi' = \frac{\partial\mathcal{H}}{\partial\rho_x} \approx \Delta\nu$. With a linear passage, we find that Φ depends quadratically on θ: $\Phi \sim \Delta\nu'\theta^2$, and this results in a Fresnel integral. This was first pointed out by Schoch[57]. Instead of $\int d\theta = \Delta\theta$, we have

$$\Delta\theta \to \int \sin\Phi d\theta = \sqrt{\frac{2\pi}{\left|\frac{d\Delta\nu}{d\theta}\right|}} = 2\pi \left(\frac{d\Delta\nu}{dn}\right)^{-1/2} \tag{6.55}$$

and thus the effective number of turns for crossing the resonance is $\left(\frac{d\Delta\nu}{dn}\right)^{-1/2}$.

6.5.3 Walkinshaw Resonance

This is $\nu_x - 2\nu_z = 0$, named for W. Walkinshaw who discovered its importance[63]. It is driven by fields proportional to xz^2 as arise from a sextupolar component. But with $m = 0$, it is the average component around the whole orbit, and so is an intrinsic independent of whether and how many sectors there are in the cyclotron. In cyclotrons that do not use stripping for extraction, the radial tune ν_x is often decreased near extraction to increase orbit separation, and so this resonance is then difficult to avoid there.

The Hamiltonian with sextupolar field can be written

$$\mathcal{H} = \frac{1}{2}(p_x^2 + p_z^2) + \frac{1}{2}(\nu_x^2 x^2 + \nu_z^2 z^2) + \frac{1}{6} a_0 (x^3 - 3xz^2). \tag{6.56}$$

The x^3 term is important for the resonance $3\nu_x = m$. This has negligible effect unless m is a multiple of the number of sectors, in which case it is an intrinsic. So the first occurrence is near $\gamma \approx N/3$ and N is usually chosen to avoid it altogether. Not so with the Walkinshaw resonance which requires only a zeroth harmonic of the magnetic field, to drive it.

The normalized field derivative a_0 is from the notation of eqn. 6.46: $\frac{R^2}{B}\frac{\partial^2 B}{\partial R^2}$. In this smooth approximation, we also have the approximation that the tune $\nu_x \approx \sqrt{1 + \frac{R}{B}\frac{\partial B}{\partial R}}$, so we can write more simply

$$a_0 = 2\nu_x \frac{d\nu_x}{dR}, \tag{6.57}$$

Often it occurs near extraction where it can compromise beam size leading to loss on the septum. An interesting example is the MSU K1200 superconducting cyclotron[64]. For high intensity machines, it can couple radial oscillations to vertical and thus cause activation.

For this case, in the preceding theory, we have $n_x = 1$, $n_z = 2$, $m = 0$, and thus

$$\mathcal{H}(\rho_x, \Phi; \theta) = -\Delta\nu\rho_x - \kappa\sqrt{\rho_x}(1 - \rho_x)\cos\Phi \tag{6.58}$$

For plotting, though, it is clearer if we plot directly the (noncanonical) normalized betatron amplitude $A_x = \sqrt{\rho_x}$ on a polar plot which is then the (x, p_x) plane. In fact just adding a constant, the expression can be factorized, which makes its character clearer:

$$\mathcal{H} = (1 - A_x^2)(\Delta\nu - \kappa A_x \cos\Phi). \tag{6.59}$$

Contours of constant $\mathcal{H}$ have been plotted in Fig. 6.6. This image needs some explaining. The plane is not to be understood as containing a distribution of particles, but each particle has its own such plane scaled according to its initial amplitude combined as $J_0 = 2J_{x0} + J_{y0}$. $A_x = \sqrt{\frac{2J_x}{J_0}}$. The outer circle is $A_x = 1$, meaning that the z-amplitude is zero. $A_x > 1$ is thus non-physical. A particle on the circle (where $\mathcal{H} = 0$ will travel clockwise until it reaches the vertex where the circle meets the vetical contour. This is one of two unstable fixed points. Slight deviation inward (meaning finite z-amplitude) will cause it to descend the vertical contour ($x = \Delta\nu/\kappa$ where $\mathcal{H} = 0$ also, see eqn. 6.59). This non-conservation of x-amplitude is compensated by a gain in z-amplitude. Exactly on resonance, all the action goes to vertical motion and then comes back into horizontal. Physically, this means a particle with motion mainly in the x-plane will eventually oscillate in the z-plane, even if the initial z-amplitude is very small. In the limit of zero J_{y0}, the time needed to transfer motion from x to z is infinite.

There is a nice demonstration of this effect on the completely analogous mechanical case of an elastic pendulum where the bouncing frequency is exactly twice the swinging frequency. Starting it bouncing vertically (x is vertical for this case), eventually results in horizontal

motion no matter how small is the initial horizontal swinging. One can find these on the web. Search "elastic pendulum" or "swinging spring".

Within the stopband $|\Delta\nu| < \kappa$, there are two stable fixed points with $p_x = 0$; exactly on resonance, these are at $A_x = \pm 1/\sqrt{3}$. (This is left as an exercise to the reader.) Particles that have a mixture of horizontal and vertical action follow other of the contours and also eventually pass through the x axis, gaining various amounts of vertical amplitudes and then losing them again. In a cyclotron, the resonance is traversed leaving the proportions of emittances disrupted. In order for the resonance to have minimal effect, it must be passed through sufficiently quickly, $\frac{d\nu}{d\theta} \gg \kappa$. An interesting study that demonstrates the emittance exchange (or rather action exchange, since the experiment used a coherent oscillation) was performed by the Argonne group on the storage ring Aladdin[65]. Marti measured the effect a coherent radial oscillation in the MSU superconducting cyclotron passing through the Walkinshaw resonance[66]. The resulting beam split vertically.

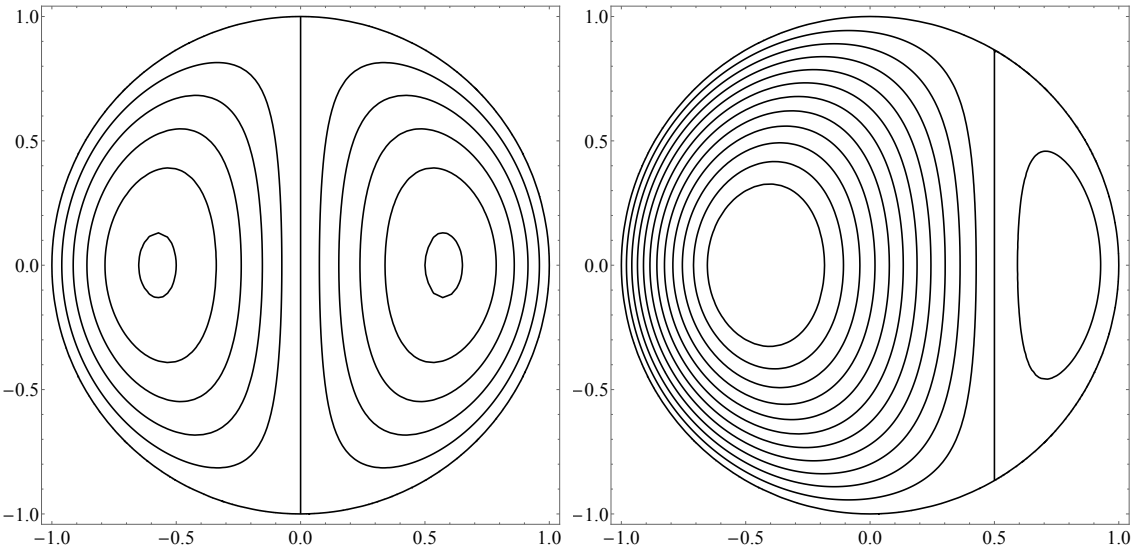

Figure 6.6: Contours of constant $\mathcal{H}$ for the Walkinshaw case, plotted on the normalized x phase plane. On the left, $\Delta\nu = 0$, on the right, $\Delta\nu = \kappa/2$. Notice that the vertical straight line contour occurs at $A_x = \Delta\nu/\kappa$; for $\Delta\nu > \kappa$, there is no x-z coupling. This is not to be understood as a phase plane populated by beam particles, since the normalization is different for each particle. See text.

Exercise 1: Show that exactly on resonance, the two stable fixed points with $p_x = 0$ are at $A_x = 1/\sqrt{3}$, $\Phi = 0, \pi$. Show further that for $x_0' = y_0' = 0$, this means initial amplitudes are in the ratio $z_0/x_0 = 2\sqrt{2}$. Plotting z versus x, one sees it traces out a (sideways) parabola instead of the normal Lissajous figure resulting from two non-synchronous sinusoids. As

x reaches max, z alternates between its max and min; when x is min, z is crossing zero. Find the equation of the parabola. Ans: $x = 2x_0\left[\left(\frac{y}{y_0}\right)^2 - \frac{1}{2}\right]$.

Exercise 2: For a cyclotron with $\frac{\partial^2 \overline{B}}{\partial R^2}$ given by that needed for isochronism, find the maximum growth rate of motion in the z-plane due to the Walkinshaw resonance if it occurs at $\nu_x = \gamma$, $\nu_z = \gamma/2$.

Note that cyclotrons (aka 'FFA's) of the EMMA type[30], consisting as they do of quadrupoles only, are in principle linear and so do not suffer from a strong the Walkinshaw resonance. Effectively, they sacrifice good isochronism to obtain linearity.

6.5.4 Linear Coupling

The intrinsic resonance $\nu_x = \nu_z$ can result in complete exchange of emittances from one plane to the other. Imagine a radially oscillating particle that receives a small vertical kick at each turn. If the tunes are equal these kicks will always have the same sign as the existing deflection, thus causing it to grow. An interesting synchrotron example is the FNAL booster. It was designed to have acceptance 2.25 times larger in the horizontal plane than the vertical[67]. But the tune split $\nu_x - \nu_z$ is so small that the planes couple resulting in a round beam and machine acceptance equal in both planes[68]. This intrinsic resonance, $m = 0$, is easily avoided in cyclotrons: they usually have $\nu_x > \nu_z$ by at least an integer.

$\nu_x - \nu_z = 1$

So the primary concern is $\nu_x - \nu_z = 1$. This depends upon a first harmonic of a radial field in the intended median plane, or in other words, a tilt or twist of the median plane, similar to adding a small skew quadrupole to a synchrotron lattice.

The part of the vertical force on an orbitting particle due to a small radial field component B_R, found simply from the Lorentz force law, is $\Delta dp_z/dt = qvB_R$ or $\Delta p_z' = qRB_R$ or $\Delta z'' = \frac{B_R R^2}{(B\rho)}$ (primes are derivatives with respect to θ). But a steady radial magnetic field component simply shifts the closed orbit vertically: $z'' + \nu_z^2 z = \frac{B_R R^2}{(B\rho)}$, which has closed orbit solution $\Delta z = \frac{B_R R^2}{\nu_z^2 (B\rho)}$. The coupling occurs if the radial field varies radially:

$$\Delta z'' = \frac{R^2}{(B\rho)} \frac{\partial B_R}{\partial R} x \tag{6.60}$$

Similarly, since $\nabla \cdot \vec{B} = 0$, we find

$$\Delta x'' = \frac{R^2}{(B\rho)} \frac{\partial B_R}{\partial R} z \tag{6.61}$$

In the notation of eqn. 6.13, we have $\delta B = \frac{\partial B_R}{\partial R} z$, or the perturbed part of the Hamiltonian in notation of eqn. 6.46 is

$$\mathcal{H}_1 = a_1 x z \cos(\theta - \theta_0) \tag{6.62}$$

where

$$a_1 = \frac{R^2}{(B\rho)} \frac{1}{2\pi} \int \frac{\partial B_R}{\partial R} \cos(\theta - \theta_0) d\theta. \tag{6.63}$$

The coupling strength κ is very simple in this case, as with the half-integer resonance, which also is linear, it does not depend upon the betatron amplitudes.

$$\kappa = \frac{a_1}{2\sqrt{\nu_x \nu_z}} \tag{6.64}$$

And the Hamiltonian for normalized action ρ_x is very similar to the Walkinshaw case:

$$\mathcal{H}(\rho_x, \Phi; \theta) = -\Delta\nu\rho_x - \kappa\sqrt{\rho_x}\sqrt{\rho_z}\cos\Phi = -\Delta\nu\rho_x - \kappa\sqrt{\rho_x}\sqrt{1-\rho_x}\cos\Phi \tag{6.65}$$

This gives contours very similar to Fig. 6.6. The difference in real space is that the fixed points are orbits that are straight lines, tilted such that the amplitude ratio of vertical to horizontal is the square root of the ratio of horizontal to vertical tunes.

As stated above, the resonance is not strictly an unstable one, since emittance is simply exchanged between planes. However, if the criterion is to allow motions to remain independent, for example to allow collimation of the vertical plane to avoid spills, the maximum amplitude growth per turn is still of interest. For normalized amplitudes, it is $d\sqrt{\rho_z}/d\theta = \kappa\sqrt{\rho_x}/2$, so unnormalized, per turn n it is

$$\left|\frac{dA_z}{dn}\right|_{\max} = \pi\sqrt{\frac{\nu_x}{\nu_z}}\kappa A_x = \frac{\pi}{2}\frac{a_1}{\nu_z}A_x \tag{6.66}$$

As with the 1-dimensional case, the overall growth is found by integrating the $\cos\Phi$ factor, and as shown by Guignard[43], it results in a Fresnel integral and, assuming in the worst case A_x not changing appreciably,

$$\Delta A_z = \frac{a_1 A_x}{4\nu_z} \left(\frac{d\Delta\nu}{dn}\right)^{-1/2}. \tag{6.67}$$

Here, $\Delta\nu = \nu_x - \nu_z - 1$.

A well-measured cyclotron may have both the axial and radial components of the magnetic field surveyed on a polar grid. In that case, calculation of the Fourier component of the radial field derivative is straightforward. But the effect can also be estimated using beam data obtained from a radial probe, instead of field data. Filtering out any coherent vertical motion, which occurs directly at the frequency of the vertical tune, the local median plane height can be measured versus radius, at preferably at least 3 locations so that the first harmonic of the local tilt can be inferred. This tilt angle itself can be used to find a_1.

Let α_1 be the tilt angle, then the median plane is a distance $z_t = \mathcal{R}\alpha(\theta) = \mathcal{R}\alpha_1 \cos(\theta - \theta_1)$ around the orbit at $\mathcal{R}$ from the geometric plane. The smoothed equations of motion can be found from the radial magnetic field, or directly from the tilt as it means simply that x, z are replaced by their rotated values: $\tilde{x} = x\cos\alpha(\theta) + y\sin\alpha(\theta)$, $\tilde{y} = -x\sin\alpha(\theta) + y\cos\alpha(\theta)$. Placing these into the unperturbed smoothed equations $(x,z)'' + \nu_{x,z}(x,z) = 0$, and keeping only first order in α, we find:

$$x'' + \nu_x^2 x = \alpha(\nu_x^2 - \nu_z^2)z \tag{6.68}$$

$$z'' + \nu_z^2 z = \alpha(\nu_x^2 - \nu_z^2)x, \tag{6.69}$$

giving

$$a_1 = \alpha_1(\nu_x^2 - \nu_z^2) \tag{6.70}$$

Exercise: The TRIUMF cyclotron reaches this resonance when $\nu_x = 1.2$ and $\nu_z = 0.2$, at 150 MeV, where the average magnetic field on orbit is 4 kG. The radial magnetic field components are roughly 0.5 Gauss and vary both azimuthally and radially on a scale of about 0.5 m. Estimate the vertical closed orbit distortion from these facts, and find an estimate of a_1 and the growth rate of the vertical amplitude.

The cure for this resonance is a first harmonic radial field of appropriate phase and amplitude to correct it. In large cyclotrons, there are "harmonic coils". They are segmented azimuthally and radially. They are in pairs; above and below the median plane. Run at the same current, they can give a first harmonic B_z, and run in opposition, they create a radial field B_r.

Bibliography

[1] M. Humbel, S. Adam, A. Adelmann, and H. Fitze, *Experience with and theoretical limits of high intensity high brightness hadron beams accelerated by cyclotrons*, in AIP Conference Proceedings, vol. 773, American Institute of Physics, 2005, pp. 313–317.

[2] E. Lawrence, *Method and apparatus for the acceleration of ions*, Feb. 20 1934. US Patent 1,948,384.

[3] K. Brown, *A first-and second-order matrix theory for the design of beam transport systems and charged particle spectrometers, SLAC 75*, 1971.

[4] H. Bethe and M. Rose, *The maximum energy obtainable from the cyclotron*, Physical Review, 52 (1937), p. 1254.

[5] L. Thomas, *The paths of ions in the cyclotron I. Orbits in the magnetic field*, Physical Review, 54 (1938), p. 580.

[6] E. Courant, M. Livingston, and H. Snyder, *The strong-focusing synchroton—a new high energy accelerator*, Physical Review, 88 (1952), p. 1190.

[7] T. Kitagaki, *A focusing method for large accelerators*, Physical Review, 89 (1953), p. 1161.

[8] D. Kerst, L. W. Jones, K. Symon, and K. Terwilliger, *A fixed field alternating gradient accelerator with spirally ridged poles*, Mid-Western Universities Research Association, internal report MURA-042, 1954.

[9] K. Symon, D. Kerst, L. Jones, L. Laslett, and K. Terwilliger, *Fixed-field alternating-gradient particle accelerators*, Physical Review, 103 (1956), p. 1837.

[10] J. Botman, M. Craddock, C. Kost, and J. Richardson, *Magnet Sector Design for a 15-GeV Superconducting Cyclotron*, IEEE Trans. Nucl. Sci. (Proc. PAC'83), 30 (1983), pp. 2007–2009.

[11] W. Joho, *ASTOR, concept of a combined acceleration and storage ring for the production of intense pulsed or continuous beams of neutrinos, pions, muons, kaons and neutrons*, IEEE Trans. Nucl. Sci. (Proc. PAC'83), 30 (1983), pp. 2083–2085.

[12] T. Zhang, S. An, T. Bian, F. Guan, M. Li, S. Pei, C. Wang, F. Wang, and Z. Yin, *A New Solution for Cost Effective, High Average Power (2 GeV, 6 MW) Proton Accelerator and its R&D Activities*, in Proc. Cyclotrons '19, no. 22 in International Conference on Cyclotrons and their Applications, JACoW Publishing, Geneva, Switzerland, jun 2020, pp. 334–339. https://doi.org/10.18429/JACoW-Cyclotrons2019-FRA01.

[13] J. Martin, *The separated-orbit cyclotron*, IEEE Trans. Nucl. Sci. (Proc. Cyc. '66), 13 (1966), pp. 288–298.

[14] U. Trinks, W. Assmann, and G. Hinderer, *The Tritron: A superconducting separated-orbit cyclotron*, Nuclear Instruments and Methods in Physics Research Section A: Accelerators, Spectrometers, Detectors and Associated Equipment, 244 (1986), pp. 273–282.

[15] A. Cazan, P. Schutz, and U. Trinks, *Commissioning of the First Separated Orbit Cyclotron Triton*, in Cyclotrons and their applications. Proceedings, 15th International Conference, Cyclotrons'98, Caen, France, June 14-19, 1998, 1999, p. C04.

[16] R. Baartman, *Synchrotronbetatron resonance driven by dispersion in rf cavities: a revised theory*, TRIUMF, internal report TRI-DN-K40, 1988.

[17] E. Courant and H. Snyder, *Theory of the alternating gradient synchrotron*, Annals of Physics, 3 (1958), pp. 1–48. [Annals Phys.281,360(2000)].

[18] K. Symon, *Applied Hamiltonian Dynamics*, in The Physics of particle accelerators: Based in part on USPAS seminars and courses in 1989 and 1990. Vol. 1, 2, vol. 249, AIP Publishing, 1992, pp. 277–377.

[19] T. Hart, D. Summers, and K. Paul, *Magnetic Field Expansion Out of a Plane: Application to Inverse Cyclotron Muon Cooling*, arXiv preprint arXiv:1105.2754, (2011).

[20] M. Gordon, *Computation of closed orbits and basic focusing properties for sector-focused cyclotrons and the design of* `CYCLOPS`, Particle Accelerators, 16 (1984), pp. 39–62.

[21] M. Gordon and T. Welton, *Computation Methods for AVF Cyclotron Design Studies*, Oak Ridge National Lab, internal report ORNL-2765, 1959.

[22] M. Berz, *Computational aspects of optics design and simulation: Cosy infinity*, Nuclear Instruments and Methods in Physics Research, 298 (1990), pp. 473–479.

[23] G. Mackenzie and C. Meade, *The Vertical Equilibrium Orbit Option (modified* `CYCLOP`*)*, TRIUMF, internal report TRI-DN-72-10, 1972.

[24] G. Mackenzie, *Some Changes Made in the Field Analysis Programs* `POLICY` *and* `CYCLOPS` *– Part 1: Interpolation and Smoothing*, TRIUMF, internal report TRI-DN-70-45, 1970.

[25] C. Meade, *Changes to the Main Magnet Code*, TRIUMF, internal report TRI-DN-70-54 Addendum 4, 1971.

[26] W. Joho, *Cyclotron specials*. Talk, available on the web, 2011.

[27] R. Louis, G. Dutto, and M. Craddock, *Central Region Orbit Dynamics in the TRIUMF Cyclotron*, IEEE Trans. Nucl. Sci. (Proc. PAC'71), 18 (1971), pp. 282–286.

[28] M. Gordon, *Canonical treatment of accelerated orbits in sector-focused cyclotrons*, Particle Accelerators, 14 (1983), pp. 119–137.

[29] T. Suzuki, *Synchrobetatron resonance driven by dispersion in RF cavities*, Part. Accel., 18 (1985), pp. 115–128.

[30] S. Machida et al., *Acceleration in the Linear Non-Scaling Fixed-Field Alternating-Gradient Accelerator EMMA*, Nature Phys., 8 (2012), pp. 243–247.

[31] M. Craddock, E. Blackmore, G. Dutto, C. Kost, G. Mackenzie, and P. Schmor, *Improvements to the Beam Properties of the TRIUMF Cyclotron*, IEEE Trans. Nucl. Sci. (Proc. PAC'77), 24 (1977), pp. 1615–1617.

[32] W. Joho, *Application of the phase compression-phase expansion effect for isochronous storage rings*, Part. Accel., 6 (1974), pp. 41–52.

[33] M. Gordon, *Some useful invariants and a transfer matrix for the longitudinal motion*, in Proc. of the 10th Int. Conf. on Cyclotrons and their Applications, East Lansing, USA, 1984, pp. 279–287.

[34] K. Symon and A. Sessler, *Methods of radio frequency acceleration in fixed field accelerators with applications to high current and intersecting beam accelerators*, CERN, internal report, 1956.

[35] M. Gordon, *Effects of spiral electric gaps in superconducting cyclotrons*, Nuclear Instruments and Methods, 169 (1980), pp. 327–336.

[36] J. R. Richardson and M. Craddock, *Beam quality and expected energy resolution from the triumf cyclotron.*, in Fifth International Cyclotron Conference (1969), R. McIlroy, ed., Univ. of British Columbia, Vancouver, London Butterworths, 1971, pp. 85–94.

[37] R. Baartman, *Cyclotron Primary Achromaticity*, TRIUMF, internal report TRI-DN-10-05, 2010.

[38] A. W. Chao, *Lectures On Accelerator Physics*, World Scientific, 2020.

[39] M. Nagaenko, Y. P. Severgin, and I. Shukejlo, *Compensation of nonlinear disturbances of isochronous mode of the moscow meson factory proton storage ring*, D.V. Efremov Scientific Research Institute of Electrophysical Equipment, internal report, 188631 Leningrad, USSR, 1987.

[40] J. Berg, *Amplitude dependence of time of flight and its connection to chromaticity*, Nuclear Instruments and Methods in Physics Research Section A: Accelerators, Spectrometers, Detectors and Associated Equipment, 570 (2007), pp. 15–21.

[41] E. Pozdeyev, *CYCO and SIR: New Tools for Numerical and Experimental Studies of Space Charge Effects in the Isochronous Regime*, PhD thesis, Michigan State University, 2003.

[42] W. Kleeven, *Theory of accelerated orbits and space charge effects in an AVF cyclotron*, PhD thesis, Technische Universiteit Eindhoven, 1988.

[43] G. Guignard, *A General Treatment of Resonances in Accelerators*, CERN Yellow Report, 78-11 (1978).

[44] W. Joho, *Extraction of a 590 MeV Proton Beam from the SIN Ringcyclotron*, PhD thesis, Swiss Federal Institute of Technology, Zurich, 1970.

[45] J. Moser, *Stabilitatsverhalten kanonischer differentialgleichungssysteme*, Nachrichten der Akademie der Wissenschaften - Gottingen IIa, 6 (1955), p. 87.

[46] T. Planche, *Designing Cyclotrons and Fixed Field Accelerators From Their Orbits*, in Proc. Cyclotrons'19, no. 22 in International Conference on Cyclotrons and their Applications, JACoW Publishing, Geneva, Switzerland, jun 2020, pp. 353–357. https://doi.org/10.18429/JACoW-Cyclotrons2019-FRB01.

[47] R. Baartman, *Linearized Equations of Motion in Magnet with Median Plane Symmetry*, TRIUMF, internal report TRI-DN-05-06, 2005.

[48] A. Garren, D. Judd, L. Smith, and H. Willax, *Electrostatic deflector calculations for the berkeley 88-inch cyclotron*, Nuclear Instruments and methods, 18 (1962), pp. 525–547.

[49] R. Baartman, G. Mackenzie, and M. Gordon, *Amplitude growth from the rapid traversal of a half-integer resonance*, in Tenth international conference on cyclotrons and their applications, 1984.

[50] R. Baartman, T. Planche, and Y.-N. Rao, *Correction of the $\nu_r = 3/2$ Resonance in TRIUMF Cyclotron*, Conf. Proc. C, 1205201 (2012), pp. 415–417.

[51] J. Bolduc, *Field tolerances associated with some resonances in the triumf cyclotron*, PhD thesis, University of British Columbia, 1972.

[52] T. Planche, Y. Rao, and R. Baartman, *Improvement of the current stability from the TRIUMF cyclotron*, CYC13, Vancouver, Canada, (2013), pp. 16–20.

[53] W. Kleeven and S. Zaremba, *Cyclotrons: magnetic design and beam dynamics*, CERN Yellow Reports: School Proceedings Archives, 1 (2017), pp. 177–239.

[54] R. Baartman, G. Mackenzie, R. Laxdal, and R. Lee, *Beam Optics for a 12-GeV Isochronous Ring Cyclotron*, IEEE Trans. Nucl. Sci. (Proc. PAC'83), 30 (1983), pp. 2010–2012.

[55] R. Hagedorn, *Stability and amplitude ranges of two dimensional non-linear oscillations with periodical Hamiltonian applied to betatron oscillations in circular particle accelerators. 1 & 2*, CERN Yellow Report, (1957).

[56] R. Hagedorn and A. Schoch, *Stability and amplitude ranges of two-dimensional non-linear oscillations with periodical Hamiltonian applied to betatron oscillations in circular particle accelerators. 3.*, CERN Yellow Report, 57-14 (1957).

[57] A. Schoch, *Theory of linear and non-linear perturbations of betatron oscillations in alternating-gradient synchrotrons*, CERN Yellow Report, (1958).

[58] D. Korteweg, *Sur certaines vibrations d'ordre supérieur et d'intensité anomale, vibrations dans les mécanismes à plusiers degrés de liberté*, Arch. Nederl. Sci. Exactes et Natur., Sér. 2, 1 (1898), pp. 229–260.

[59] H. Beth, *The oscillations about a position of equilibrium where a simple linear relation exists between the frequencies of the principal vibrations (second part)*, Koninklijke Nederlandse Akademie van Wetenschappen Proceedings Series B Physical Sciences, 12 (1909), pp. 735–750.

[60] H. Beth, *The oscillations about a position of equilibrium where a simple linear relation exists between the frequencies of the principal vibrations (third part)*, Koninklijke Nederlandse Akademie van Wetenschappen Proceedings Series B Physical Sciences, 13 (1910), pp. 742–761.

[61] H. Meier and K. Symon, *Analytical And Computational Studies On The Interaction Of A Sum And A Difference Resonance*, in 2nd International Conference on High-Energy Accelerators, 1959, pp. 253–263.

[62] G. Guignard, *Selection of formulae concerning proton storage rings*, CERN Yellow Report, 77-10 (1977).

[63] J. Burren, N. King, and W. Walkinshaw, *Coupled motion in the spiral ridge cyclotron*, Atomic Energy Research Establishment, internal report T/R 2342, Harwell, Didcot, Berkshire, UK, 8 1957.

[64] M. Gordon, F. Marti, and X. Wu, *Effects on a beam of prolonged weaving around the $\nu_r = 2\nu_z$ resonance*, in Eleventh international conference on cyclotrons and their applications, 1987, pp. 252–255.

[65] J. Liu, E. Crosbie, L. Teng, J. Bridges, K. Symon, and W. Trzeciak, *Difference resonance study on the electron storage ring Aladdin at SRC*, Argonne National Lab., IL (United States), internal report LS-183, 1995.

[66] F. Marti and S. Snyder, *Internal Beam Dynamics Studies with a TV Probe*, in Cyclotrons and their applications: Proceedings, 13th International Conference, Vancouver, Canada, July 6-10, 1992, 1993, pp. 435–438.

[67] E. Hubbard (editor), *Booster Synchrotron*, FNAL, internal report TM-0405, 1973.

[68] M. McAteer, S. Kopp, and E. Prebys, *Measurement and manipulation of beta functions in the fermilab booster*, in 2011 PAC Conf. Proc., 2011, pp. 1579–1581.